



# RF accelerating structures, Lecture 8

Vyacheslav Yakovlev

**PHY862 “Accelerator Systems”**

September 21, 2023

**MICHIGAN STATE**  

---

**UNIVERSITY**

# RF accelerating structures

## Outline:

4. Periodic acceleration structures;
5. Standing –Wave acceleration structures;
6. Why SRF cavities?

# Chapter 4.

## Periodic acceleration structures.

- a. Coupled cavities and periodic structure;
- b. Travelling waves in a periodic structure;
- c. Dispersion curve;
- d. Phase and group velocities;
- e. Parameters of the TW structures;
- f. Equivalent circuit for a travelling – wave structure;
- g. Losses in the TW structure;
- h. Types of the TW structures;
- i. Examples of modern TW structures.

# Periodic acceleration structures:

- Single – cell cavities are not convenient to achieve high acceleration: a lot of couplers, tuners, etc.
- Especially it is important for electron acceleration:

$R_{sh} = R/Q \cdot Q_0 \sim \omega^{1/2}$ , low Ohmic losses at high frequency;  
 $v=c$ , focusing is quadratic and does not depend on frequency.



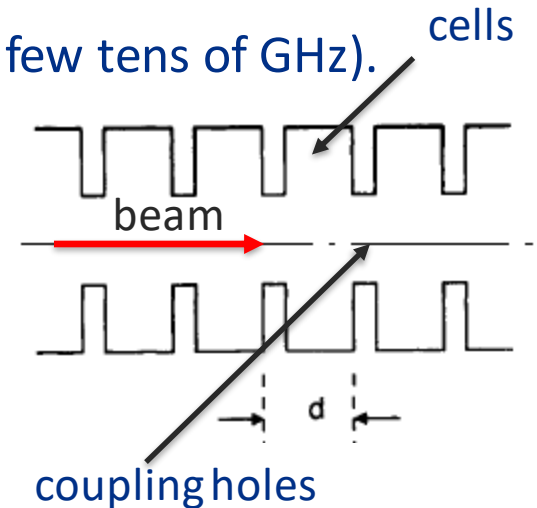
high frequencies are preferable (typically up to few tens of GHz). cells



small cavity size,  $\sim 1$  cm for RT,  $\sim 20$  cm for SRF



periodic structure of coupled cells.



- To provide synchronism with the accelerated particle, the particle velocity  $v_p = \beta c = v_{ph} = \omega / k_z$  and the structure period  $d = \varphi / k_z = \varphi \lambda / (2\pi\beta)$ ;  $\varphi$  is phase advance per period,  $\varphi = k_z d$ .

# Periodic acceleration structures:

- Each previous cell excites EM field in a current cell, which in turn excites the field in the next cell.

- Cavity excitation by surface tangential electric field:

$$\vec{E}_j = \sum_0^\infty X_{ij} \vec{E}_j - \text{field in the } j^{\text{th}} \text{ cell;}$$

$\vec{E}_j$  - eigen functions of cells.

- Single-mode approximation:

$$\vec{E}_j = X_j \vec{E}_0 - \text{field in the } j^{\text{th}} \text{ cell. Works everywhere except the hole}$$

$\vec{E}_0$  - eigen function of the operation  $TM_{010}$  mode of a cell.

- Excitation of a cavity by the field of a similar neighboring cavity through a small hole:

- Boundary conditions for the excited cavity field  $\vec{E}$  :  $E_t = 0$  on  $S$ ;  $E_t = \mathbf{E}$  on  $S_1$  (hole). For eigenfunction  $E_{0t} = 0$  on  $S + S_1$

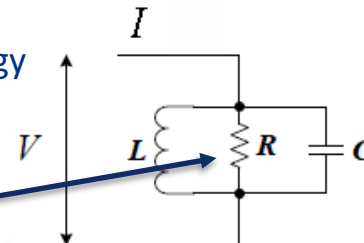
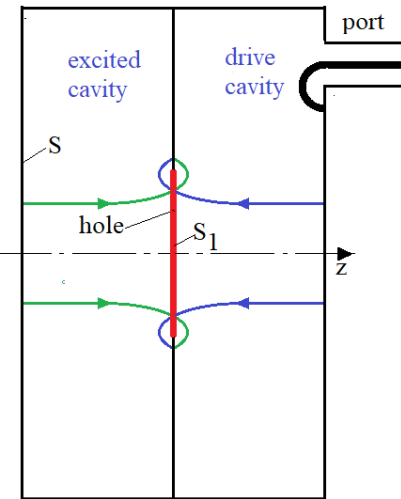
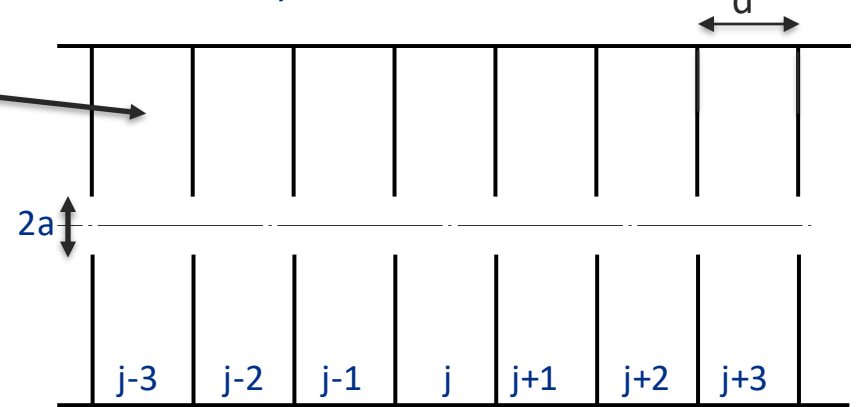
- From Maxwell equations for eigenfunction and excited field:

$$X = \frac{\int_{S_1} \vec{E} \times \vec{H}_0 dS}{2\omega W \left(1 - \frac{\omega_0^2}{\omega^2}\right)}, \text{ here } \vec{H}_0 \text{ is eigen magnetic field, } W \text{ - stored energy}$$

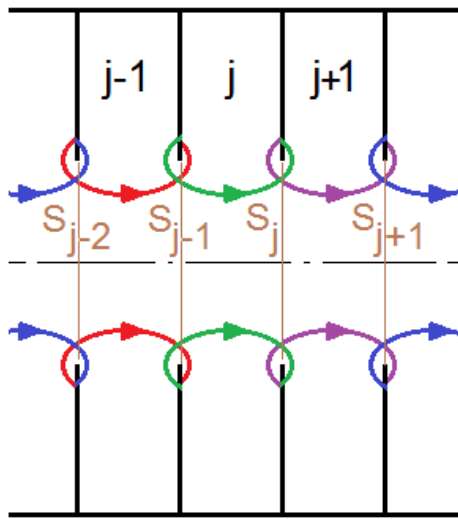
$\omega_0$  - eigen frequency,  $\omega$  - drive frequency.

(Exact derivation is in the Appendix 11)

Amplitude X is the same as for a parallel oscillator



# Periodic acceleration structures:

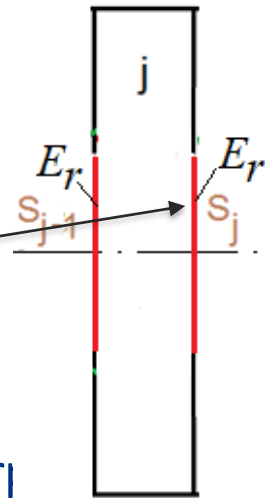


In the  $j^{\text{th}}$  cell  $\vec{E}_j = X_j \vec{E}_0$

Excitation of a cavity by surface electric field:

$$X_j = \frac{\int_{S_{j-1}} \vec{E}_{j-1} \times \vec{H}_0 dS}{2\omega W \left(1 - \frac{\omega_0^2}{\omega^2}\right)} + \frac{\int_{S_j} \vec{E}_j \times \vec{H}_0 dS}{2\omega W \left(1 - \frac{\omega_0^2}{\omega^2}\right)} \quad (1)$$

On the coupling holes tangential electric is superposition of the fields of the current cell and the neighboring cell:



$$\int_{S_{j-1}} \vec{E}_{j-1} \times \vec{H}_0 dS = K \frac{\omega_0^2}{\omega} W (X_j - X_{j-1}), \quad \int_{S_j} \vec{E}_j \times \vec{H}_0 dS = K \frac{\omega_0^2}{\omega} W (X_j - X_{j+1}), \quad (2)$$

here  $K = \frac{\omega}{W\omega_0^2} \int_S \vec{E}_0 \times \vec{H}_0 dS$  - dimensionless constant depending on the cavity shape.

Therefore, from (1) and (2) one has:

$$X_j \left(1 - \frac{\omega_0^2}{\omega^2}\right) - \left(K \frac{\omega_0^2}{\omega^2} X_j - \frac{1}{2} K \frac{\omega_0^2}{\omega^2} X_{j-1} - \frac{1}{2} K \frac{\omega_0^2}{\omega^2} X_{j+1}\right) = 0,$$

or

$$X_j \left(1 - (1 + K) \frac{\omega_0^2}{\omega^2}\right) + \frac{1}{2} K \frac{\omega_0^2}{\omega^2} (X_{j-1} + X_{j+1}) = 0 \quad (1)$$

(Exact derivation is in the Appendix 11)

# Periodic acceleration structures:

- For a pillbox  $K$  depends on the aperture as  $a^3$ :
- In paraxial approximation  $E_{z0}$  for  $TM_{010}$  modes in a pillbox cavity does not depend on  $r$  in cylindrical coordinates  $\vec{r}, \vec{\varphi}, \vec{z}$ , see Lecture 8, page 46.
- In presence of a small hole radial electric field  $E_{r0} \sim r$  next to the hole.

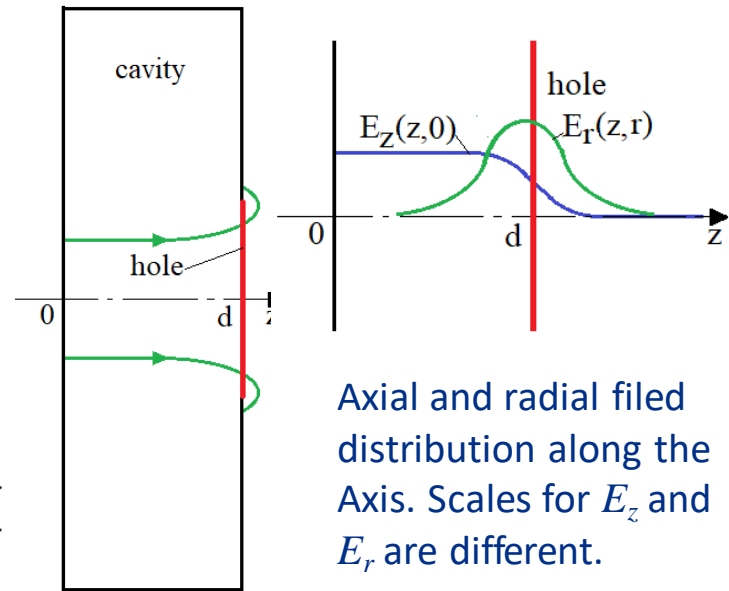
• On the other hand,  $div \vec{E} = \frac{1}{r} \frac{\partial(rE_r)}{\partial r} + \frac{\partial E_z}{\partial z} = 0 \rightarrow E_{r0}(r) = -\frac{r}{2} \frac{\partial E_z}{\partial z} \approx \frac{rE_{z0}}{4a}$ ;

$$H_{\varphi 0}(r) = \frac{1}{2i\omega a} \int_0^r E_{z0} r dr \sim r, \text{ and } \int_{S_{j-1}} E_{r0} H_{\varphi 0} dS \sim a^3$$

- For pillbox cells having thin walls and a hole with the radius  $a$  one has

$$K = \frac{2E_0^2 a^3}{3Z_0 W_0 c} = \frac{2}{3} \cdot \frac{R/Q}{Z_0} \cdot \frac{k_0 a^3}{d^2 T^2} \quad k_0 = \frac{\omega_0}{c}$$

(Exact derivation is in the Appendix 11)



Axial and radial field distribution along the Axis. Scales for  $E_z$  and  $E_r$  are different.

Pillbox cavity with a hole



## THE PHYSICAL REVIEW

*A journal of experimental and theoretical physics established by E. L. Nichols in 1893*

SECOND SERIES, VOL. 66, NOS. 7 AND 8

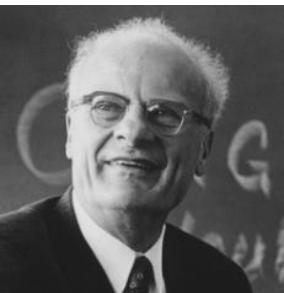
OCTOBER 1 AND 15, 1944

Theory of Diffraction by Small Holes

H. A. BETHE

Department of Physics, Cornell University, Ithaca, New York

(Received January 26, 1942)





# Travelling–Wave acceleration structures:

In the infinite chain of cavities equation  $X_j \left(1 - (1 + K) \frac{\omega_0^2}{\omega^2}\right) + \frac{1}{2} K \frac{\omega_0^2}{\omega^2} (X_{j-1} + X_{j+1}) = 0$  (1) has solution (travelling wave):

$$X_j = X e^{ij\varphi} \quad (2)$$

- From (1) and (2) it follows

$$1 = (1 + K) \frac{\omega_0^2}{\omega^2} + \frac{1}{2} K \frac{\omega_0^2}{\omega^2} (e^{i\varphi} + e^{-i\varphi})$$

or

$$\omega(\varphi) = \omega_0 [1 + K(1 - \cos\varphi)]^{1/2}$$

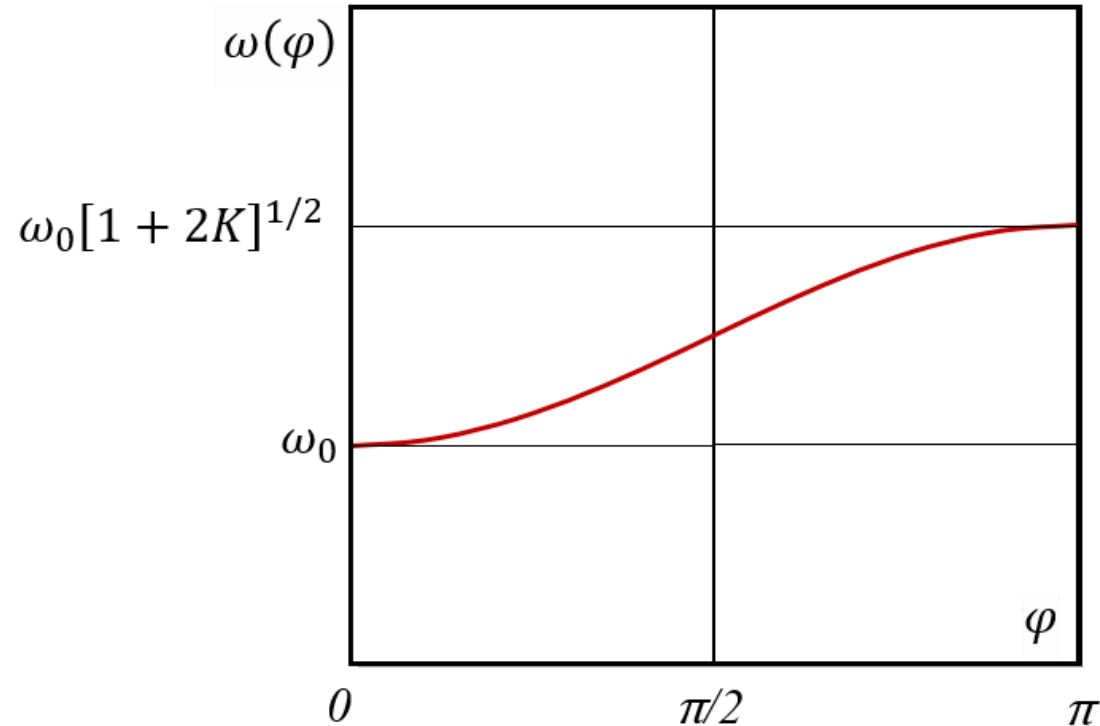
- For small  $K$  we have:

$$\omega(\varphi) \approx \omega_0 \left[1 + \frac{1}{2} K(1 - \cos\varphi)\right]$$

- One can see that

$$K = \frac{\omega(\pi) - \omega(0)}{\omega(0)} \quad \text{- a coupling coefficient; here } \omega(\pi) \approx \omega_0(1+K), \omega(0) \approx \omega_0$$

$$\Delta f = f(\pi) - f(0) \quad \text{- a passband width}$$





## Travelling–Wave acceleration structures:

- In the arbitrary infinitely long periodic structure, or in the finite structure matched on the ends, there are travelling waves (TW) having arbitrary phase shift per cell  $\varphi$ . Longitudinal wavenumber, therefore, is  $k_z = \varphi/d$ . Dispersion equation is the same:

$$\omega(k_z) \approx \omega_{\pi/2} \left( 1 - \frac{K}{2} \cos(\varphi) \right) = \omega_{\pi/2} \left( 1 - \frac{K}{2} \cos(k_z d) \right)$$

Therefore, the phase velocity  $v(\varphi)$  is:

$$v_{ph}(\varphi) = \frac{\omega(k_z)}{k_z} = c \frac{2\pi d}{\varphi \lambda}$$

- For acceleration of the particle having velocity  $v_p = \beta c$ , the cavity cell length  $d$  should be equal to

$$d = \frac{\beta \lambda \varphi}{2\pi},$$

because for synchronism we need  $v_p = v_{ph}$

For example, for  $\varphi = \pi$  the cell should have the length of  $\beta \lambda / 2$ .

# Travelling–Wave acceleration structures:

□ The group velocity\*  $v_{gr}(\varphi)$  is

$$v_{gr}(\varphi) = \frac{d\omega}{dk_z} \approx c \frac{\pi K d}{\lambda} \sin(\varphi)$$

**For  $\varphi=0$  and  $\varphi=\pi$  group velocity is zero!**

For  $\varphi=\pi/2$  group velocity is maximal:

$$v_{gr}(\pi/2) = c \frac{\pi K d}{\lambda}.$$

- For small  $K$  group velocity is small compared to the speed of light.
- In contrast to a waveguide,  $v_{ph} \cdot v_{gr} \neq c^2$ .

\*In homogeneous media  $v_{gr} = \frac{P}{w}$ ,  $P$  is power flow density,  $w$  is energy density.

# Travelling–Wave acceleration structures :



John Stewart Bell

□ For TW in a periodic structure:

- Average stored energy per unit length for electric field  $w_E$  is equal to the average stored energy per unit length for magnetic field  $w_H$  (the 1<sup>st</sup> Bell Theorem\*):

$$w_E = w_H = w/2$$

- The power  $P$  flow is a product of the average stored energy per unit length and the group velocity (the 2<sup>d</sup> Bell Theorem\*):

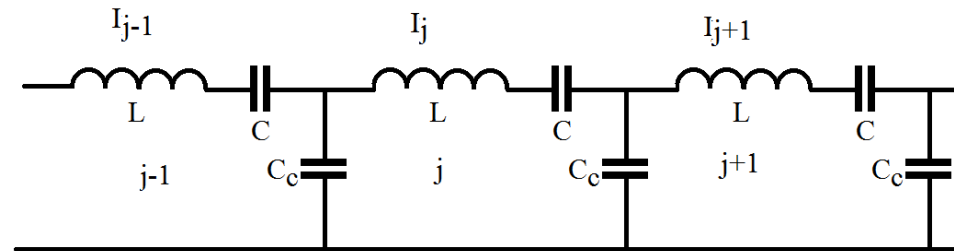
$$P = v_{gr} w.$$

*\*J.S. Bell, “Group velocity and energy velocity in periodic waveguides,” Harwell, AERE-T-R-858 (1952). See proof in Appendix 11*

# Travelling-Wave acceleration structures

Equivalent circuit:

Note that the electrodynamics in the periodic structure is described by the equivalent circuit



For  $j^{\text{th}}$  cell we have from Kirchhoff theorem:

$$\left(i\omega L + \frac{1}{i\omega C}\right)I_j + \frac{(I_j - I_{j-1})}{i\omega C_c} + \frac{(I_j - I_{j+1})}{i\omega C_c} = 0,$$

For the capacity voltage  $X_j = \frac{I_j}{i\omega C}$  we have the same equation as for EM model:

$$X_j \left[1 - (1 + K) \frac{\omega_0^2}{\omega^2}\right] + \frac{1}{2}K \frac{\omega_0^2}{\omega^2} [X_{j-1} + X_{j+1}] = 0$$

Here  $\omega_0^2 = \frac{1}{LC}$ ,  $K = \frac{2C}{C_c}$ ,  $C = \frac{2}{\omega_0 R/Q}$ ,  $L = \frac{R/Q}{2\omega_0}$ .

# Travelling-Wave acceleration structures

Loss in the cells:

Ohmic loss on the metallic surface:

$$\omega_0 \rightarrow \omega_0 \left(1 + \frac{i}{2Q_0}\right)$$



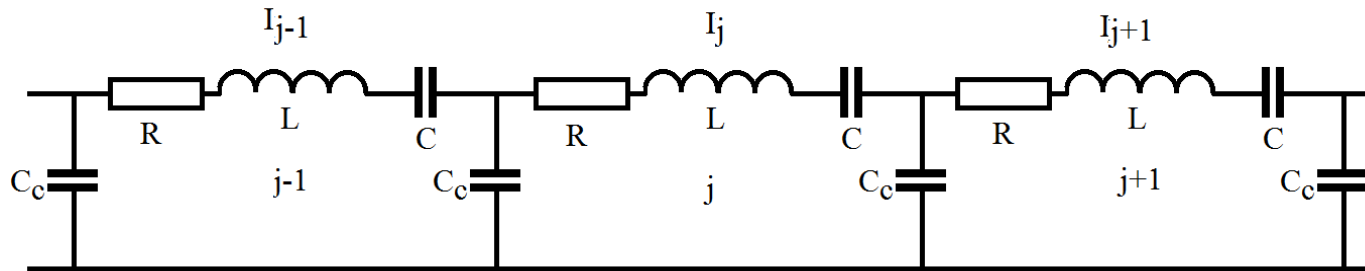
$$\vec{E}, \vec{H} \sim e^{i\omega_0 t - t/\tau} = e^{i\omega_0 t \left(1 + \frac{i}{2Q_0}\right)}$$

$$\tau = \frac{2Q_0}{\omega_0}$$

and

$$X_j \left[1 - (1 + K) \frac{\omega_0^2}{\omega^2} + i \frac{\omega_0^2}{Q_0 \omega^2}\right] + \frac{1}{2} K \frac{\omega_0^2}{\omega^2} [X_{j-1} + X_{j+1}] = 0$$

Equivalent circuit is the following:



where

$$R = \frac{R/Q}{2Q_0} \quad \omega_0^2 = \frac{1}{LC}, \quad K = \frac{2C}{C_c}, \quad C = \frac{2}{\omega_0 R/Q}, \quad L = \frac{R/Q}{2\omega_0}$$

# Travelling–Wave acceleration structures

However, in a long periodic TW structure Ohmic losses change acceleration field distribution along the structure.

Energy conservation law in the  $j^{\text{th}}$  cell:

$$\frac{dW_{0,j}}{dt} = -P_j + P_{j-1} - \frac{\omega_0 W_{0,j}}{Q_0},$$

Taking into account that  $w = \frac{W_0}{d}$  and  $P = w \cdot v_{gr}$  we have

$$\frac{\partial w}{\partial t} = - \frac{(w \cdot v_{gr}|_j - w \cdot v_{gr}|_{j-1})}{d} - \frac{\omega_0 w}{Q_0} \approx - \frac{\partial(w v_{gr})}{\partial z} - \frac{\omega_0 w}{Q_0}$$

In steady-state case we have  $\frac{dw}{dz} = - \frac{w}{v_{gr}} \left( \frac{dv_{gr}}{dz} + \frac{\omega_0}{Q_0} \right)$

- **Constant impedance structure:**

$$v_{gr} = \text{const} \rightarrow w(z) = w(0) e^{-\frac{z\omega_0}{v_{gr}Q_0}} \rightarrow E(z) = E(0) e^{-\frac{z}{v_{gr}\tau}} \quad \tau = \frac{2Q_0}{\omega_0}$$

- **Constant gradient structure:**

$$v_{gr}(z) = v_{gr}(0) - z \frac{\omega_0}{Q_0} \rightarrow w(z) = w(0) \rightarrow E(z) = E(0) = \text{const}$$

Aperture  $a$  should decrease with  $z$ .

# Travelling–Wave acceleration structures

Tolerances:

If the cell frequencies have resonant frequency deviation  $\delta\omega_0$ , it changes the longitudinal wave number  $k_z$  and violates synchronism.

$$\delta k_z = \frac{dk_z}{d\omega_0} \delta\omega_0 = \frac{1}{v_{gr}} \delta\omega_0$$

It means that it is necessary to operate in the middle of dispersion curve, when group velocity is maximal,  $\varphi \sim \pi/2 - 2\pi/3$ .

If  $\varphi$  close to  $\pi$ , the structure is unstable.



# Travelling–Wave acceleration structures

TW structure parameters:

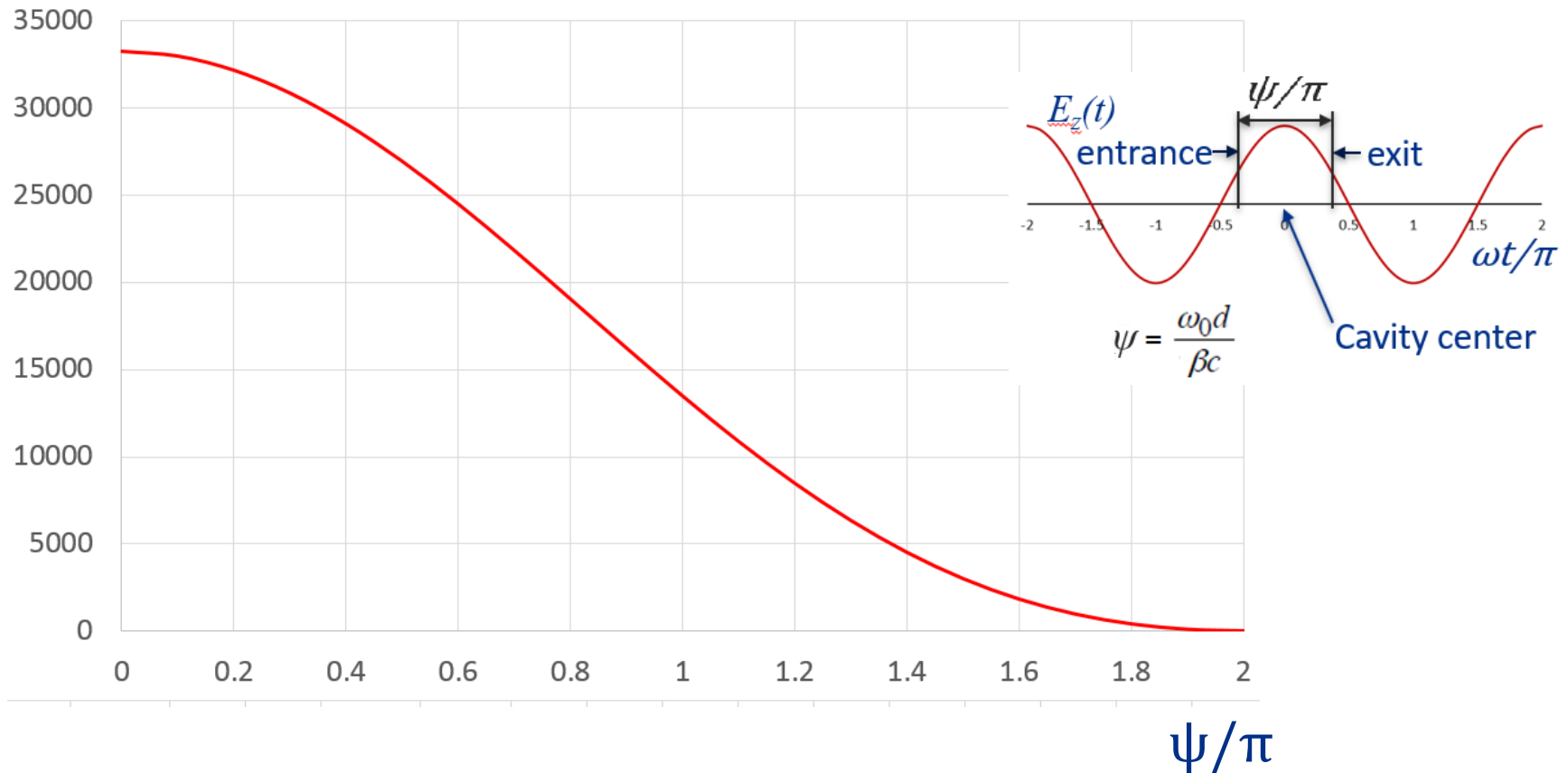
For TW structure  $R$  and  $R/Q$  are calculated per unit length of the structure.

- ❖ Shunt impedance  $R$  is measured in M $\Omega$ /m. For geometrically similar cells  $R$  scales as  $\omega_0^{1/2}$ .
- ❖  $R/Q$  is measured in  $\Omega$ /m. For geometrically similar cells  $R/Q$  scales as  $\omega_0$

# Travelling-Wave acceleration structures

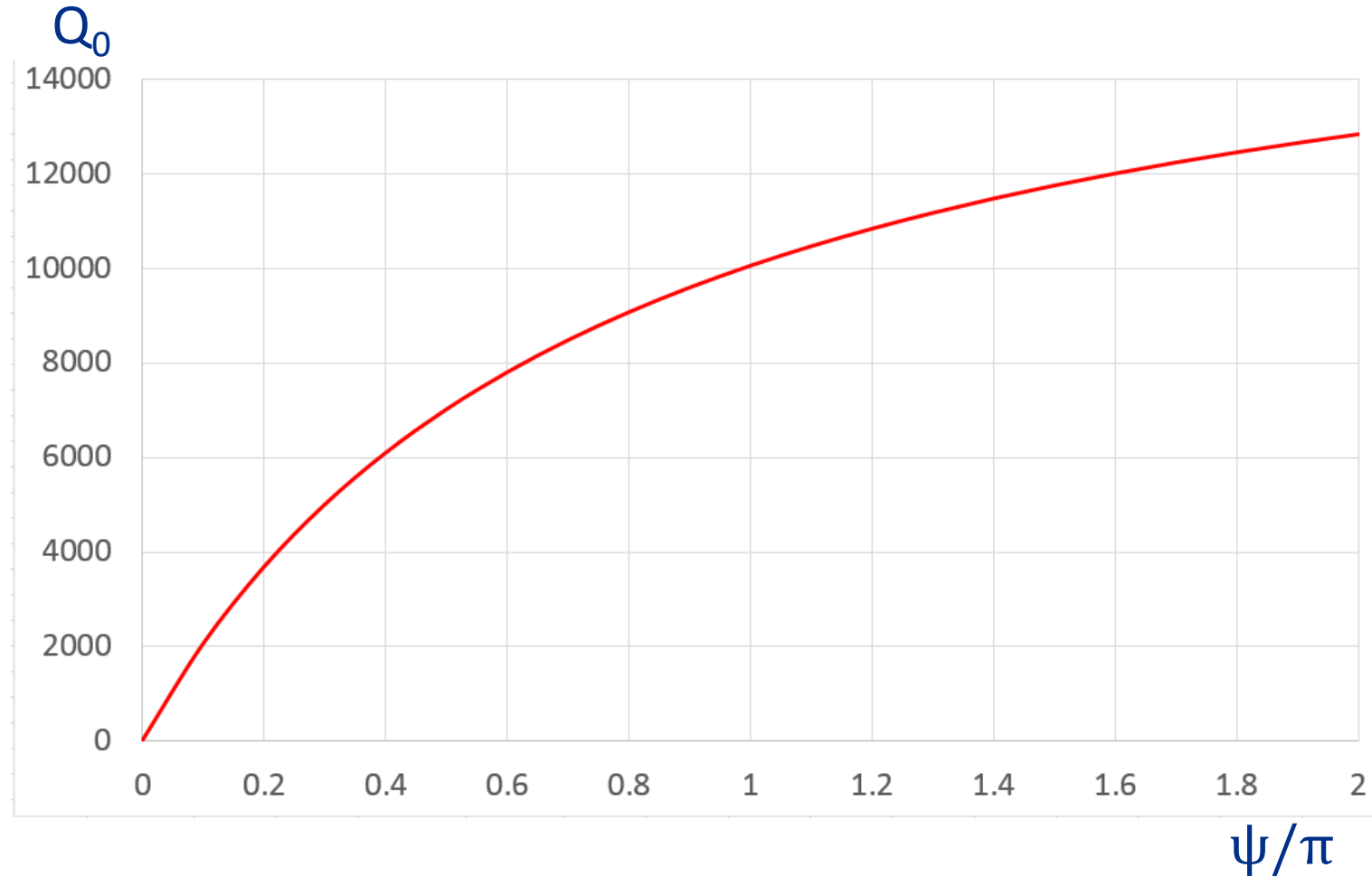
TW structure parameters:  $(R/Q)$  for pillbox,  $f=10$  GHz (here  $b$  is the cavity radius)

$R/Q$ , Ohm/m      $\frac{R}{Q} = \frac{0.98Z_0T(\psi)^2}{b}$ ,      $b = \frac{2.405c}{2\pi f}$      (See Lecture 7, slide 46)



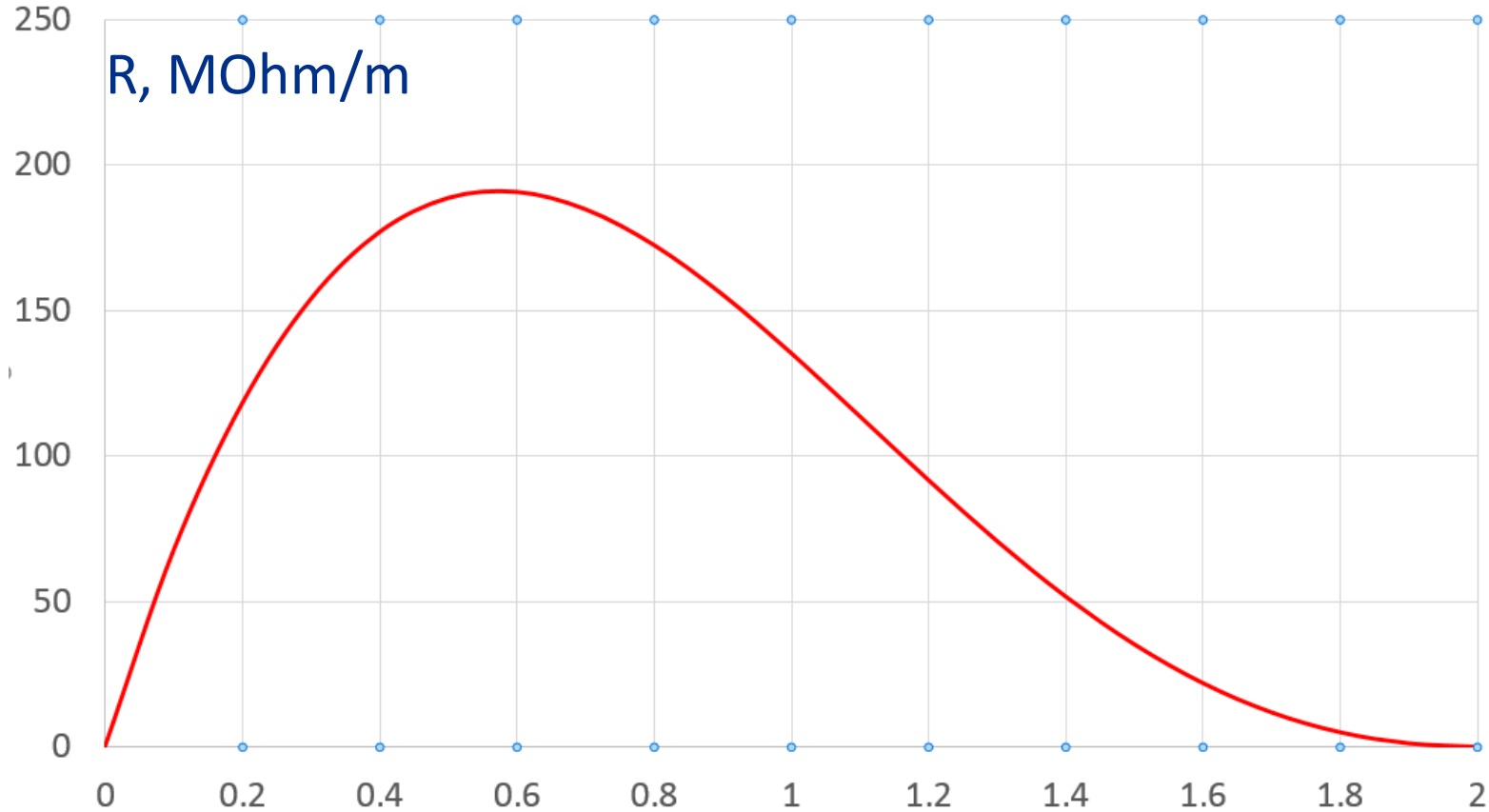
# Travelling-Wave acceleration structures

TW structure parameters:  $Q_0$  for pillbox at 10 GHz (see Lecture 7, slide 52)



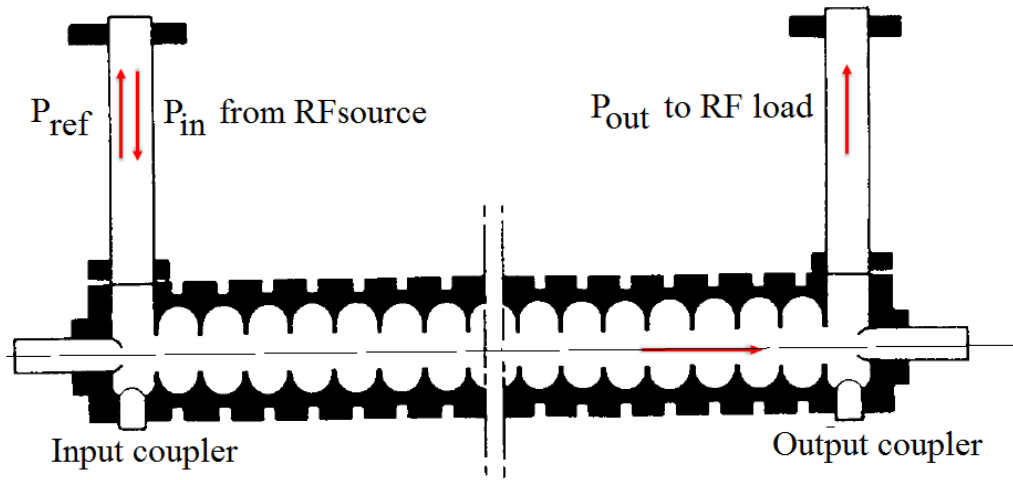
# Travelling-Wave acceleration structures

TW structure parameters: Shunt impedance  $R=(R/Q)\cdot Q_0$  for pillbox at 10 GHz



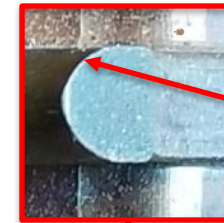
$R$  is maximal at  $\psi \sim 0.6\pi$ . Typically, they use  $\psi = 2\pi/3$ .  $\psi/\pi$

# Travelling-Wave acceleration structures

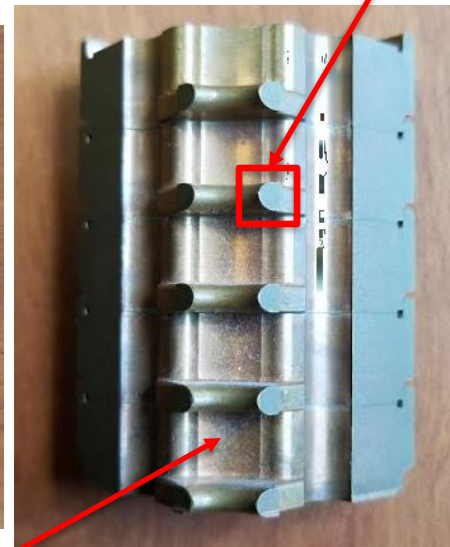
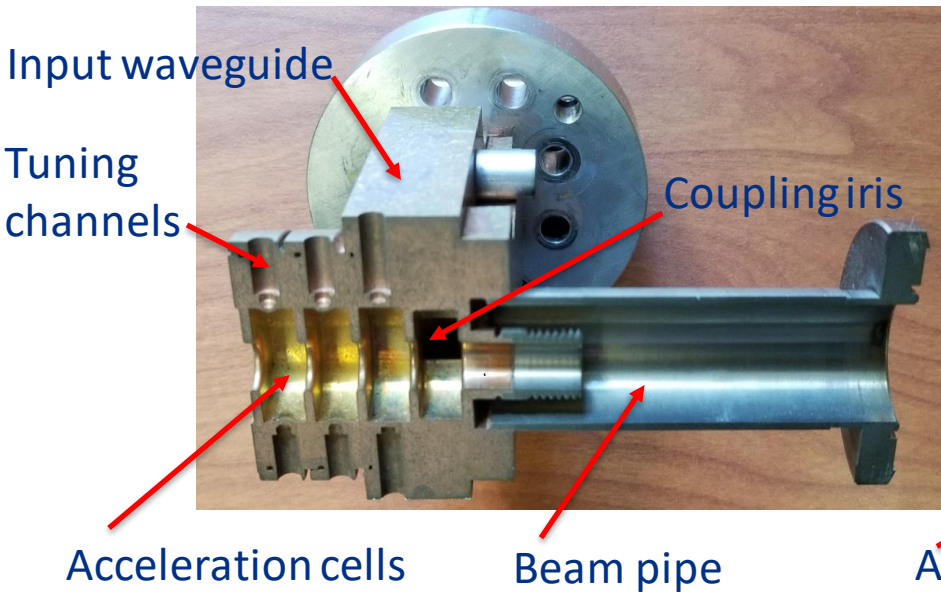


$$P_{in} = P_{ref} + P_{out} + P_{loss} + P_{beam}$$

$$P_{in} \gg P_{out}$$

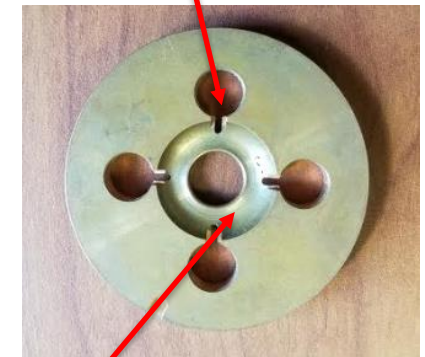


Aperture has elliptical shape to minimize surface electric field



Acceleration cells

HOM dampers



Acceleration cell  
NLC structure with  
HOM damping



# Travelling–Wave acceleration structures

TW structures for acceleration of electrons are widely used in different fields.

## ❖ High – energy physics:

- SLAC (1968): 3 km, 47 GeV (max),  $2\pi/3$  2.856 GHz (S-band) , 3 m structures.
- SLC (1987) – first  $e^+e^-$  linear collider based on the SLAC linac.
- CLIC collider (R&D): up to 50 km, up to 3 TeV c.m.,  $2\pi/3$  12 GHz

## ❖ FELS:

- SwissFEL (PSI) 5.7 GHz linac (2017), 0.74 km, 5.8 GeV,  $2\pi/3$  6 GHz

## ❖ Industrial and medical accelerators

- Varian S-band (2.856 GHz) and X-band (11.424 GHz) linacs for medical applications
- Industrial linacs

# Travelling–Wave acceleration structures

Modern TW structures: 12 GHz CLIC structure\*

## Accelerating structure parameters

Loaded gradient* [MV/m]	100
Working frequency [GHz]	11.994
Phase advance per cell	$2\pi/3$
Active structure length [mm]	217
Input/output radii [mm]	3.15/2.35
Input/output iris thickness [mm]	1.67/1.00
Q factor [Cu]	7112/7445
Group velocity [%c]	1.99/1.06
Shunt impedance [M $\Omega$ /m]	107/137
Peak input power [MW]	60.9
Filling time [ns]	49.5
Maximum E-field [MV/m]	313
Maximum modified Poynting vector [MW/mm <sup>2</sup> ]	7.09
Maximum pluse heating temperature rise [K]	35

\*V. Dolgashev, SLAC, EAAC 2015



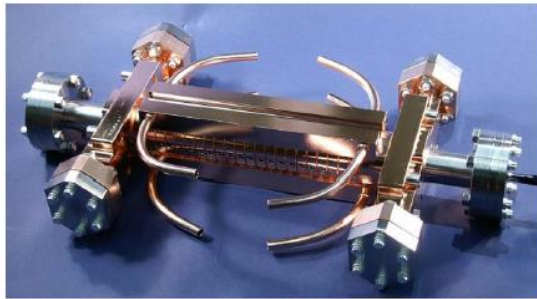
# Travelling-Wave acceleration structures

Modern TW structures: 12 GHz CLIC structure\*

Traveling Wave accelerator structures, CLIC prototypes

SLAC

T18 → TD18 → T24 → TD24



T18\_Disk\_#2

2009



undamped

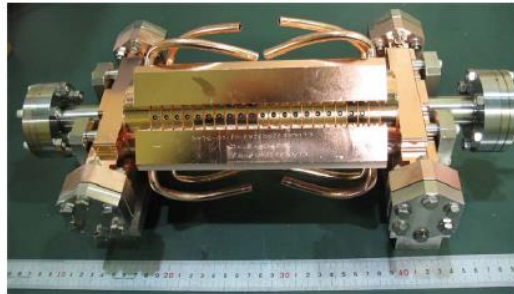


T24\_Disk\_#3

2011



2011~12

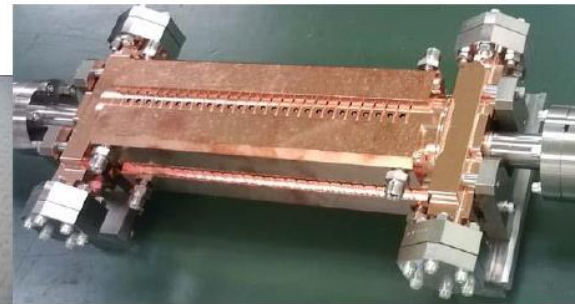


TD18\_Disk\_#2

2010



damped



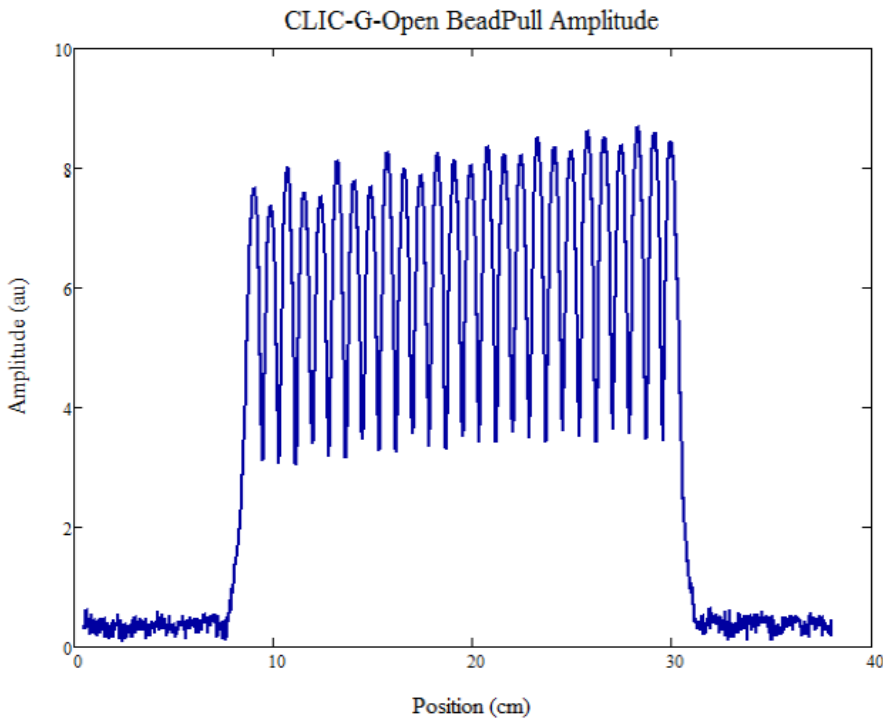
TD24\_Disk\_#4

# Travelling-Wave acceleration structures

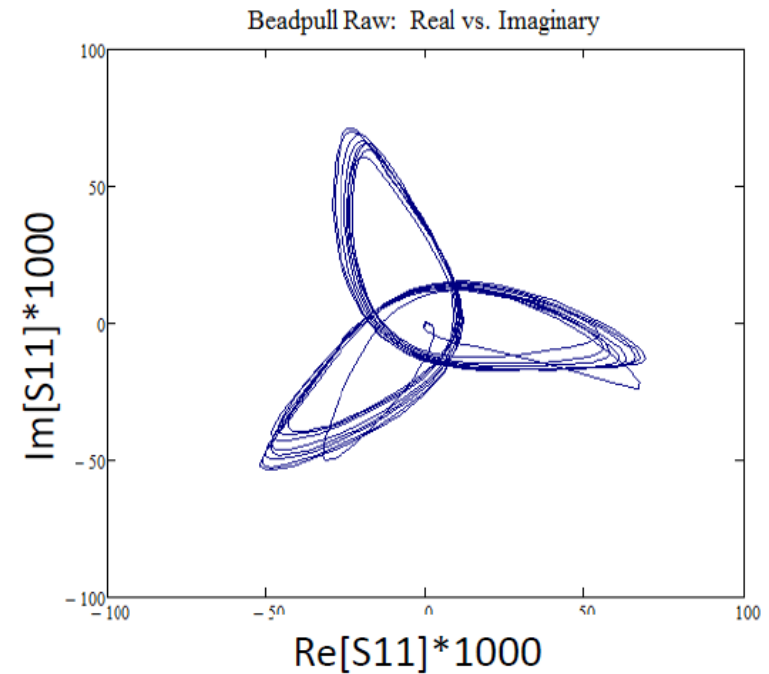
Modern TW structures: 12 GHz CLIC structure\*



## Final beadpull of tuned CLIC-G-OPEN



On-axis field amplitude.



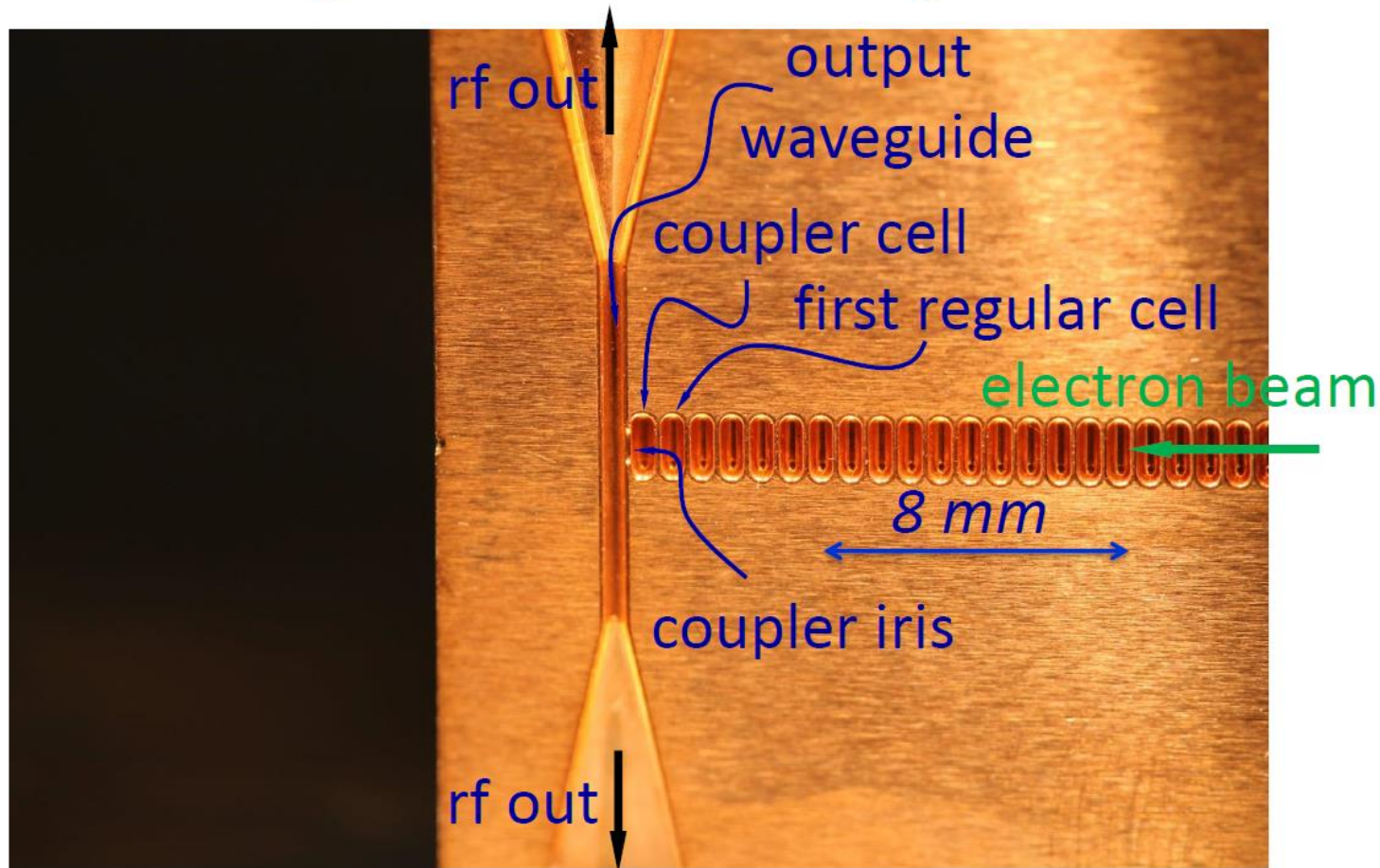
Polar plot of beadpull data.



# Travelling-Wave acceleration structures

SLAC

## Output Part of the Open 100 GHz Copper Traveling Wave Accelerating Structure



SI AC-INFN

Fermilab

# Summary:

- Single – cell cavities are not convenient in order to achieve high acceleration: a lot of couplers, tuners, etc. Especially it is important for acceleration of electrons.
- Periodic structures are used for acceleration, where travelling wave is excited.
- Phase velocity depend on the phase advance per cell. The accelerating wave has the same phase velocity as the accelerated particles (synchronism).
- Average energy of magnetic field is equal to average energy of electric field (the 1<sup>st</sup> Bell theorem); Power flow is equal to the product of the group velocity to the average stored energy per unit length (the 2<sup>d</sup> Bell theorem).
- The passband depends on the value of coupling between the cells  $K$  ; it depends on the coupling hole radius  $a$  as  $\sim a^3 - a^4$ ; it depends also on the wall thickness.
- Group velocity is maximal if phase advance per cell is  $\sim \pi/2$ ;
- Maximal shunt impedance per unit length is at the phase shift of  $\sim 2\pi/3$ ;
- Loss may change the field distribution. To achieve field flatness along the structure, group velocity (coupling) should decrease from the structure beginning to the end.

# Chapter 5.

## Standing –Wave acceleration structures.

- a. Standing - wave structures;
- b. Equivalent circuit for a SW structure;
- c. Dispersion curve;
- d. Normal modes;
- e. Perturbation theory for SW structures;
- e. Parameters of SW structures;
- f. Bi-periodic SW structures;
- g. Inductive coupling;
- h. Types of the SW structures;

# Standing-Wave acceleration structures

## ❖ TW structures work very good for RT electron accelerators:

- High frequency  $\rightarrow$  lower power ( $R \sim f^{1/2}$ );
- A lot of cells (many tens)  $\rightarrow$  high efficiency (all the power is consumed in the structure, and small fraction is radiated through the output port).

## ❖ TW structures are not good for RT proton accelerators:

- High frequency is not practical (defocusing is proportional to  $f$ )
- Low beam loading  $\rightarrow$  large number of cells (impractical from the point of view of focusing and manufacturing, especially if the cell diameter is large because of low frequency);

## ❖ TW structures are not good for SRF accelerators:

- High frequency is not practical (BCS surface resistance is proportional to  $f^2$ )
- Small decay in the cavities
- Very large number of cells + large cell size (impractical from the point of view of manufacturing and processing);
- Feedback waveguide - still under R&D

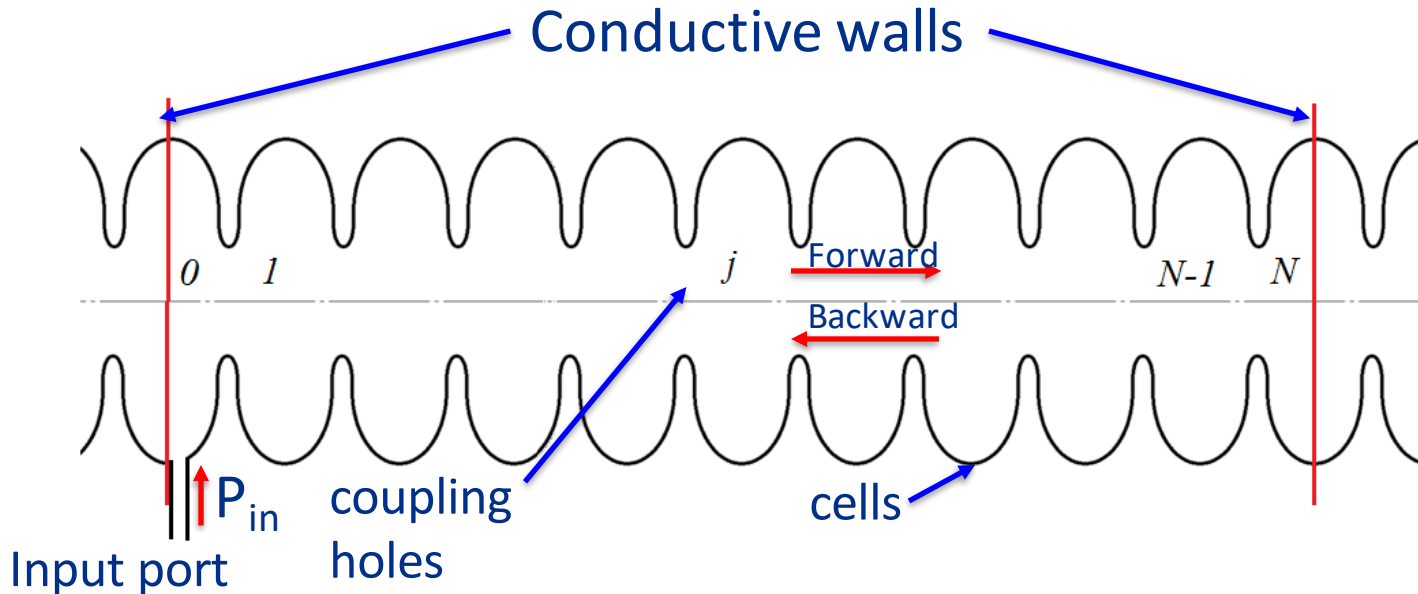
Fermilab & Euclid 3-cell SRF TW structure prototype





# Standing-Wave acceleration structures

Standing Wave structures:



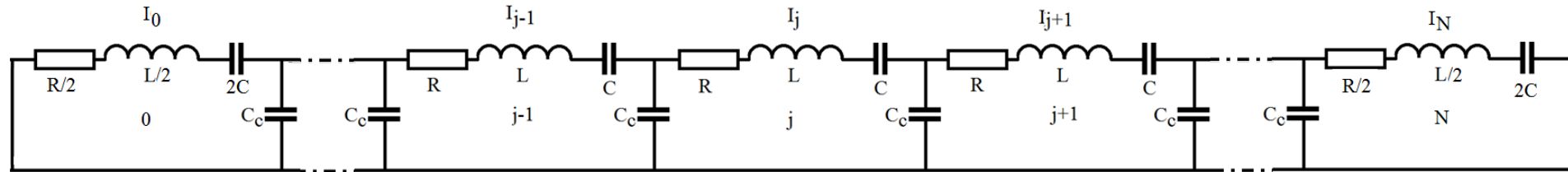
Putting reflective conductive walls in the middle of the end cells, we do not violate boundary conditions for EM field for  $TM_{010}$ -like modes.

**Forward and backward travelling waves form standing wave.**

- $N$  may be small, even  $N=2$ ;
- Frequency may be small, up to hundreds of MHz  $\rightarrow$  proton acceleration
- Suitable for SRF
- $P_{in} \ll P_{forward} \approx P_{backward}$

# Standing-Wave acceleration structures

Equivalent circuit of the SW structure containing half-cells on the ends:



$$X_0 \left[ 1 - \frac{\omega_0^2}{\omega^2} + i \frac{\omega_0^2}{Q_0 \omega^2} \right] + K \frac{\omega_0^2}{\omega^2} X_1 = 0$$

$$X_j \left[ 1 - \frac{\omega_0^2}{\omega^2} + i \frac{\omega_0^2}{Q_0 \omega^2} \right] + \frac{1}{2} K \frac{\omega_0^2}{\omega^2} [X_{j-1} + X_{j+1}] = 0 \quad (1)$$

$$X_N \left[ 1 - \frac{\omega_0^2}{\omega^2} + i \frac{\omega_0^2}{Q_0 \omega^2} \right] + K \frac{\omega_0^2}{\omega^2} X_{N-1} = 0$$

In matrix form:

$$M \hat{X} - \frac{\omega_0^2}{\omega^2} \hat{X} = 0$$

here  $M_{jj} = 1; j = 0, 1, \dots, N;$

$$M_{jj-1} = \frac{K}{2W(j)}; j = 1, 2, \dots, N;$$

$$M_{jj+1} = \frac{K}{2W(j)}; j = 0, 1, \dots, N-1.$$

and  $W(j) = 1, j = 1, 2, \dots, N-1$

$$W(j) = \frac{1}{2}, j = 0, N$$

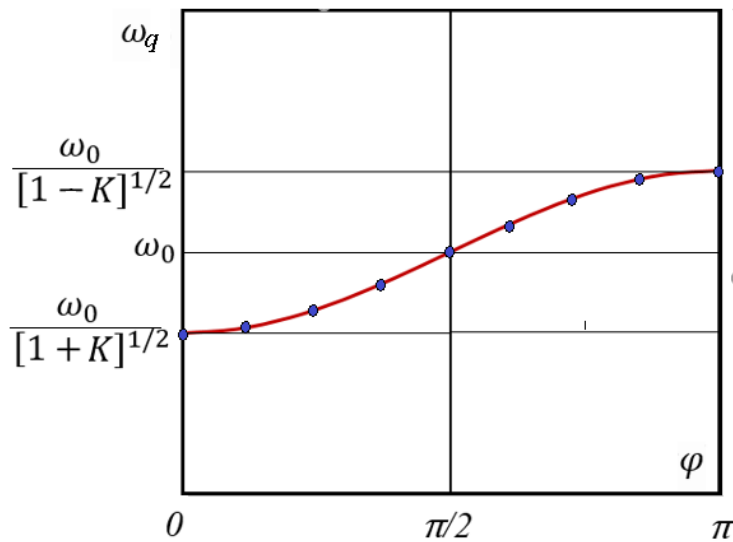
Here  $\omega_0$  corresponds to the center of dispersion curve.

# Standing –Wave acceleration structures

Eigenvectors and eigenvalues:

$$\hat{X}_j^q = \cos \frac{\pi q j}{N}; \quad \omega_q^2 = \frac{\omega_0^2}{1 + K \cos \frac{\pi q}{N}}, \quad q = 0, 1, \dots, N$$

Phase advance per cell:  $\varphi = \frac{\pi q}{N}, q = 0, 1, \dots, N$



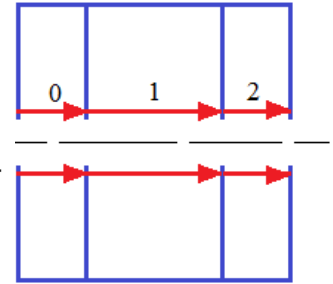
Orthogonality:

$$\hat{X}^q \cdot \hat{X}^r \equiv \sum_{j=0}^N W(j) \hat{X}_j^q \hat{X}_j^r = \frac{N \delta_{qr}}{2W(q)}, \quad \delta_{qq} = 1, \text{ and } \delta_{qr} = 0, \text{ if } q \neq r$$

3-cell cavity (N=2)

0-mode (q=0):

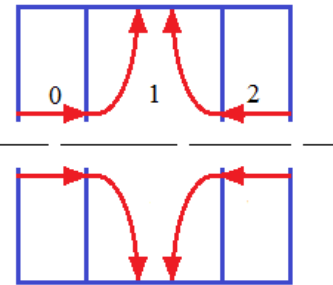
$$\varphi = 0 \quad \omega = \frac{\omega_0}{(1-K)^{1/2}}$$



$\pi/2$ -mode (q=1):

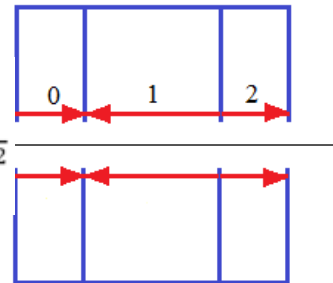
$$\varphi = \pi/2 \quad \omega = \omega_0$$

Even cell is empty!



$\pi$ -mode (q=2):

$$\varphi = \pi \quad \omega = \frac{\omega_0}{(1+K)^{1/2}}$$



# Standing –Wave acceleration structures

- Perturbation of the cell resonance frequencies causes perturbation of the mode resonance frequencies  $\delta\omega_q$ ;
- the field distribution  $\delta\hat{X}_q$ .

$$\omega_{0j}^{2'} = \omega_0^2 + \delta\omega_{0j}^2 \quad \rightarrow \quad \hat{X}^{q'} = \hat{X}^q + \delta\hat{X}^q, \quad \hat{X}^q \cdot \delta\hat{X}^q$$

Variation of the equation (1) in matrix form  $M\hat{X} - \frac{\omega_0^2}{\omega^2}\hat{X} = 0$ , see Slide 31

gives 
$$M\delta\hat{X}^q = \frac{\omega_0^2}{\omega_q^2} \left[ \delta\hat{X}^q + \Omega\hat{X}^q - \frac{\delta\omega_q^2}{\omega_q^2}\hat{X}^q \right],$$



$$\frac{\delta\omega_q^2}{\omega_q^2} = [2W(q)/N] \cdot \hat{X}^q \Omega \hat{X}^q;$$

$$\delta\hat{X}^q = \sum_{q' \neq q} \frac{2W(q')\hat{X}^q \Omega \hat{X}^{q'}}{N \left( \frac{\omega_q^2}{\omega_{q'}^2} - 1 \right)} \hat{X}^{q'}$$



$$|\delta\hat{X}^q| \sim \frac{|\delta\omega_{0j}|_{av}}{|\omega_q - \omega_{q\pm 1}|}$$

(here  $\Omega = \begin{bmatrix} \frac{\delta\omega_{01}^2}{\omega_0^2} & \dots & 0 \\ \vdots & \ddots & \vdots \\ 0 & \dots & \frac{\delta\omega_{0N}^2}{\omega_0^2} \end{bmatrix}$ )

# Standing –Wave acceleration structures

$\pi/2$ -mode ( $q=N/2$ ):  $N$ -even,  $N$  is the number of cells in the cavity

$$|\delta\hat{X}^{N/2}| \sim \frac{|\delta\omega_{0j}|_{av}}{|\omega_{N/2} - \omega_{N/2-1}|} \sim N \frac{|\delta\omega_{0j}|_{av}/\omega_0}{K}$$

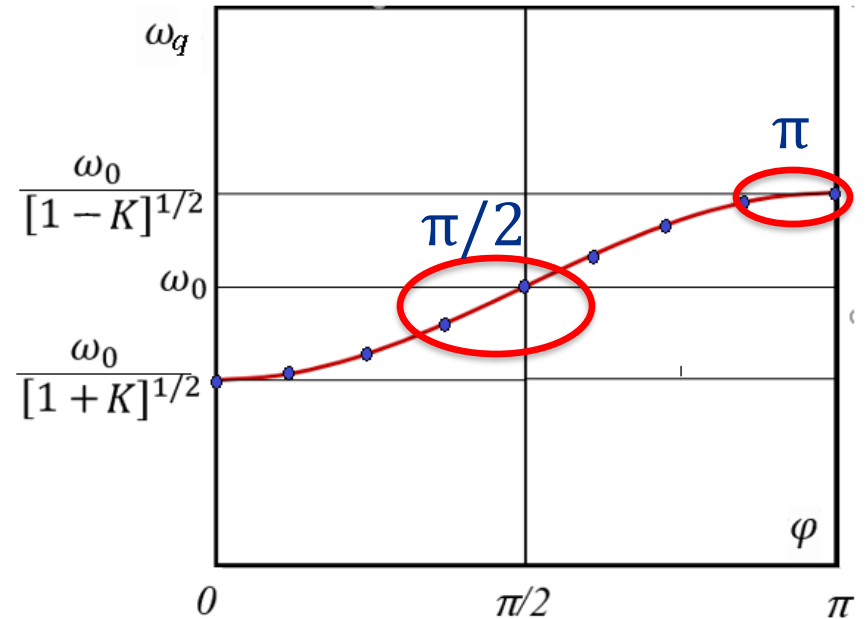
$\pi$ -mode ( $q=N$ ):

$$|\delta\hat{X}^N| \sim \frac{|\delta\omega_{0j}|_{av}}{|\omega_N - \omega_{N-1}|} \sim N^2 \frac{|\delta\omega_{0j}|_{av}/\omega_0}{K}$$

SW  $\pi$ -mode is much less stable than  $\pi/2$ -mode!

For  $\pi$ -mode problems with

- Tuning
- Temperature stability at RT



$$\omega_q^2 = \frac{\omega_0^2}{1 + K \cos \frac{\pi q}{N}}, q = 0, 1, \dots, N$$

# Standing –Wave acceleration structures

## Solutions:

- ❖ Operate at  $\pi/2$  mode;
- ❖ Operate at  $\pi$  mode:
  - Small number of cells  $N$ ;
  - Increase  $K$ .

### 1. Operating at $\pi/2$ mode:

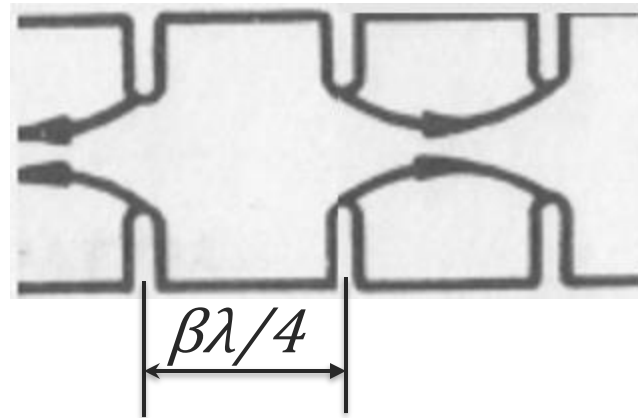
$$\hat{X}_j = \cos \frac{\pi j}{2}$$

Even cells are empty!

Solution – biperiodic structures:

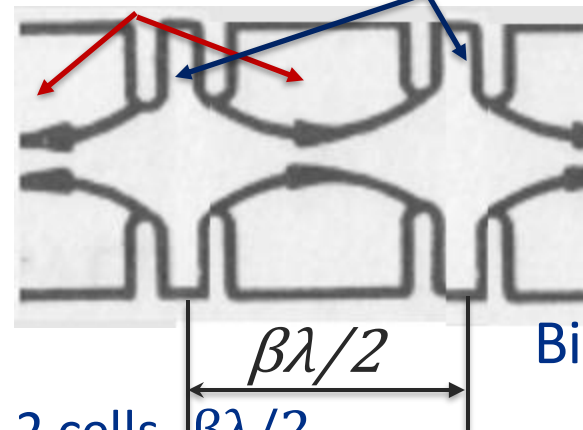
- Narrow even cells (coupling cells)
- Long odd cells (acceleration cells)
- Same length of the period containing 2 cells,  $\beta\lambda/2$
- The structure is “ $\pi/2$  for RF” and “ $\pi$  for the beam”

odd even



Periodic

Accelerating cells (odd) Coupling cells (even)

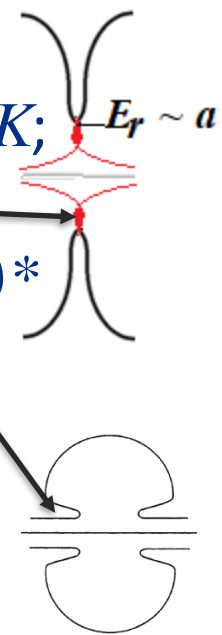


Biperiodic

# Standing –Wave acceleration structures

## 2. Increase $K$ :

- Coupling through the aperture holes does not provide high  $K$ ;
  - Aperture is limited by surface electric field
  - At  $\beta < c$  acceleration gain on the axis drops as  $\sim \exp(ka/\beta)^*$
- In this case,  $R_{sh}$  is modest (the drift tubes cannot be used)

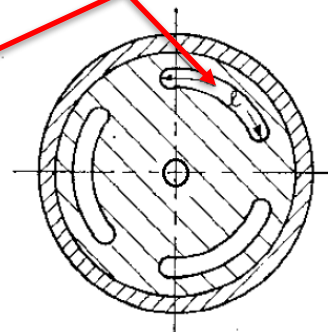
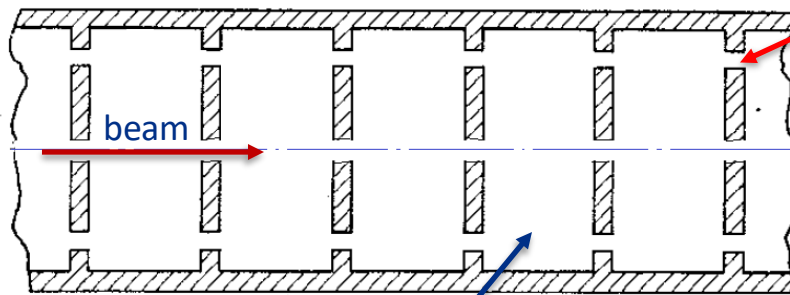


Solution: inductive coupling through the side slots.

Aperture may be small in this case, which provides

- Small field enhancement factors;
- High  $R/Q$  and  $R_{sh}$ .

Coupling slots



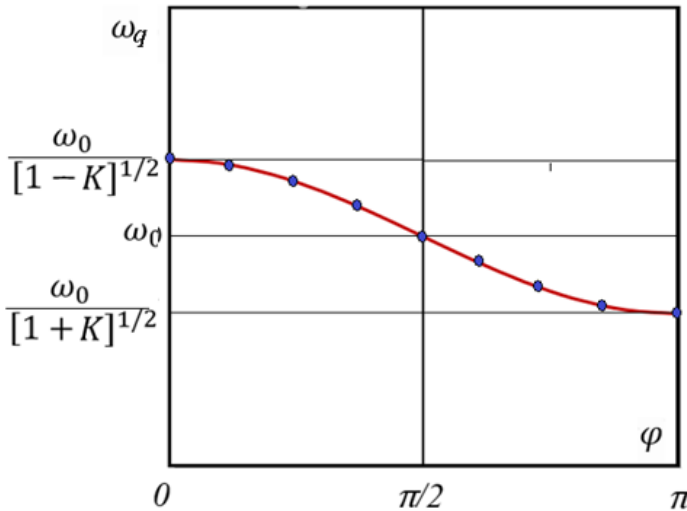
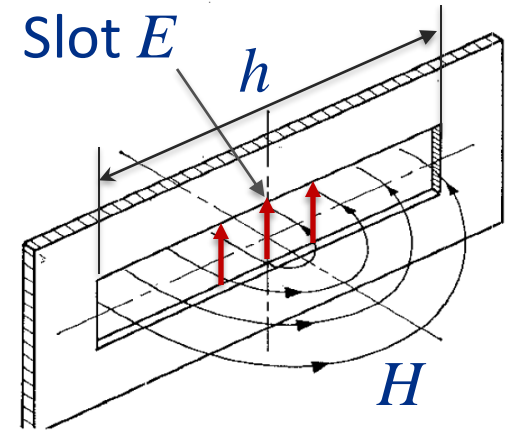
\*See Lecture 7, slide 25

Accelerating cells

# Standing-Wave acceleration structures

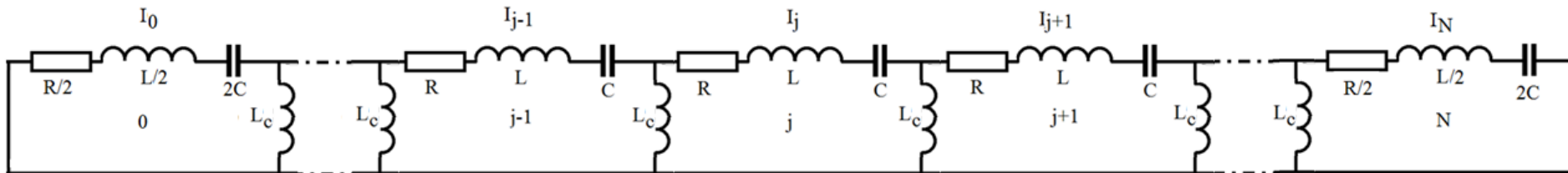
TEM wave in the slot  $\rightarrow$  high electric field  $\rightarrow$  high coupling

Induction coupling gives negative  $K$



$$K = -\frac{2L_c}{L_c}$$

Slot resonance:  $h = \lambda/2$ . Typically,  $h < \lambda/2$



Equivalent circuit below the slot resonance



# Standing-Wave acceleration structures

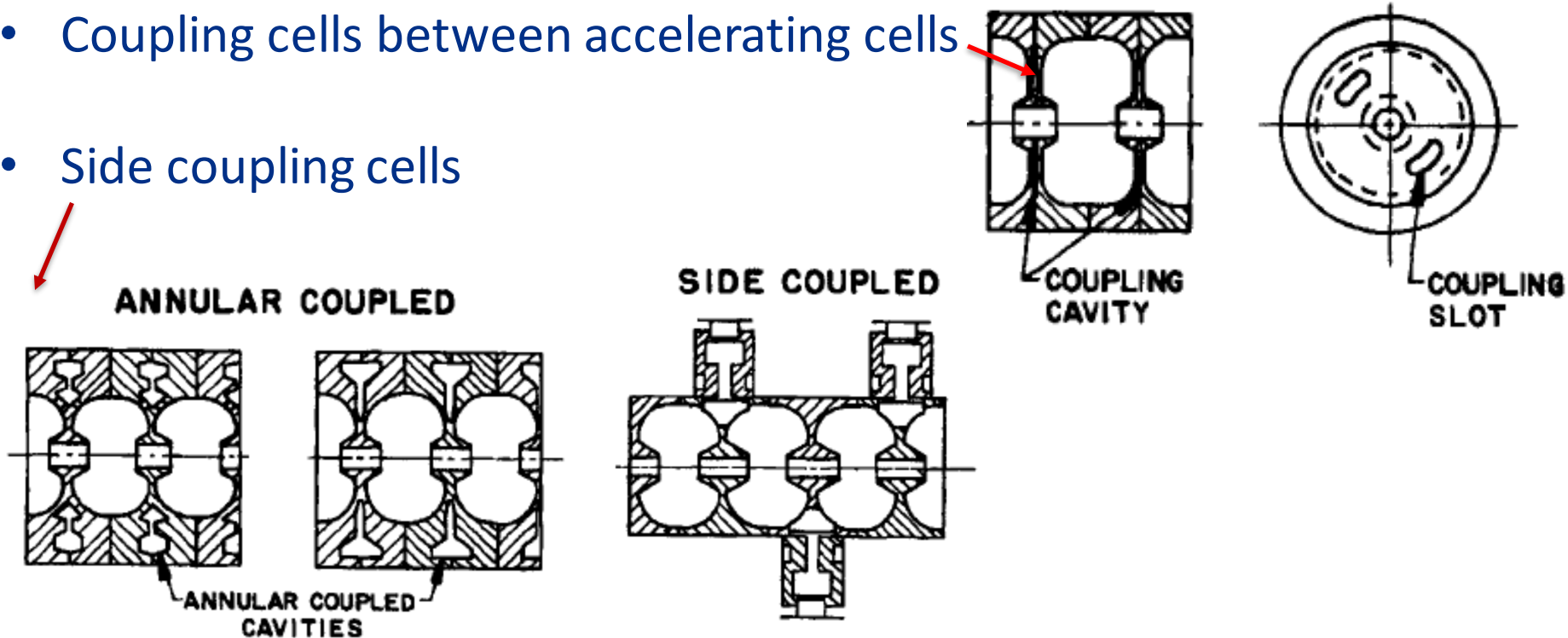
Combination:

- Inductive coupling
- Biperiodic structure



Biperiodic structures with induction coupling

- Coupling cells between accelerating cells
- Side coupling cells



# Standing-Wave acceleration structures

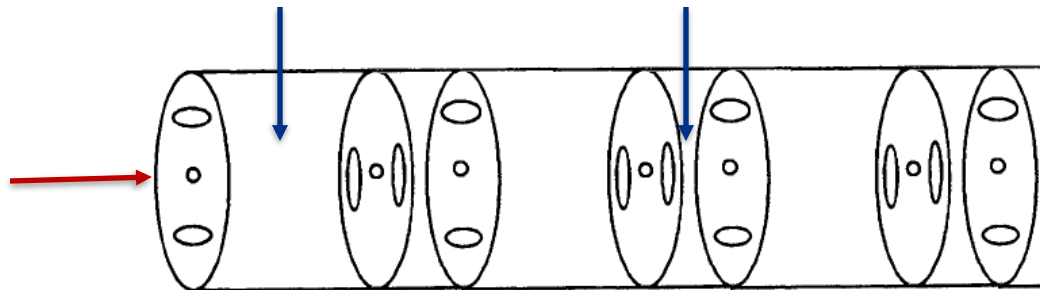
Inductive coupling slots cause multipole perturbation of the acceleration field, which may influence the beam dynamics:

$$x'_f = \frac{\Delta p_{\perp}}{p_{\parallel}} \approx \frac{m}{ka} \left( \frac{V_{max}(a)}{\gamma m_0 c^2} \right) \left( \frac{x_i}{a} \right)^{m-1}$$

Accelerating cell.

Coupling cell.

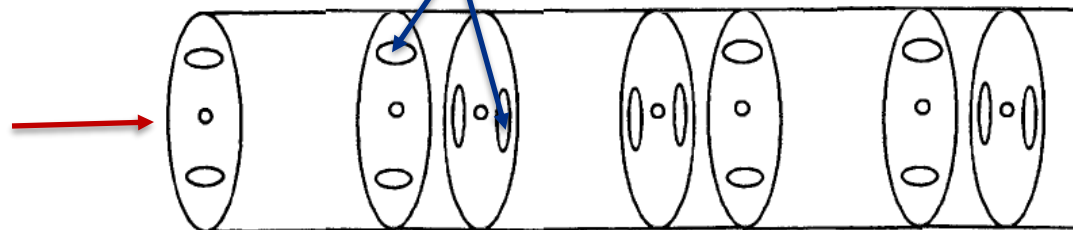
Coupling slot orientation:



Wrong! Strong quadrupole defocusing in one of transverse directions.

beam

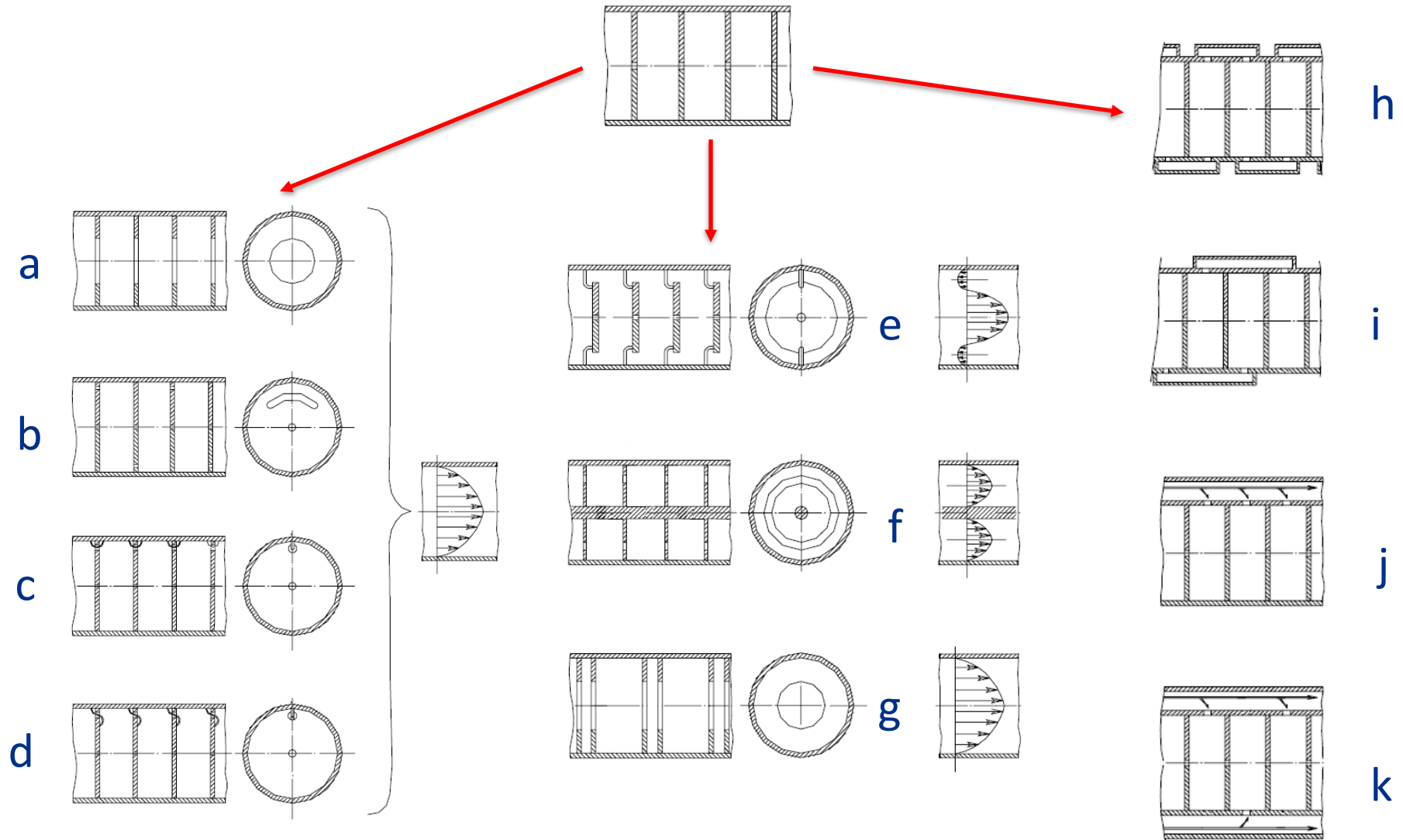
Coupling slots



Right! Strong quadrupole focusing in both directions.

# Standing-Wave acceleration structures

Different types of the RT SW acceleration structures:



# Summary:

- TW structures are not practical for RT proton accelerators (low beam loading).
- TW structures are not practical for SRF accelerators, proton and electron.
- The cure is a standing – wave structure.
- In the SW structure the operating mode is split, the number of resulting modes is equal to the number of cells.
- $\pi/2$  - mode is the most stable versus cell frequency perturbation, field distribution perturbation is proportional to the number of cells.
- 0- mode and  $\pi$ - mode are less stable versus cell frequency perturbation, field distribution perturbation is proportional to the number of cells squared, which does not allow large number of cells.
- Remedy:
  - biperiodic structures;
  - inductive coupling.

# Chapter 6.

## Why SRF cavities?

# Why SRF?

## The surface resistance

The radio-frequency surface resistance can be described in terms of three different contributions:

$$R_S(T, \omega, B, l) = R_{BCS}(T, \omega, l) + R_{fl}(B, l) + R_0$$

Where:

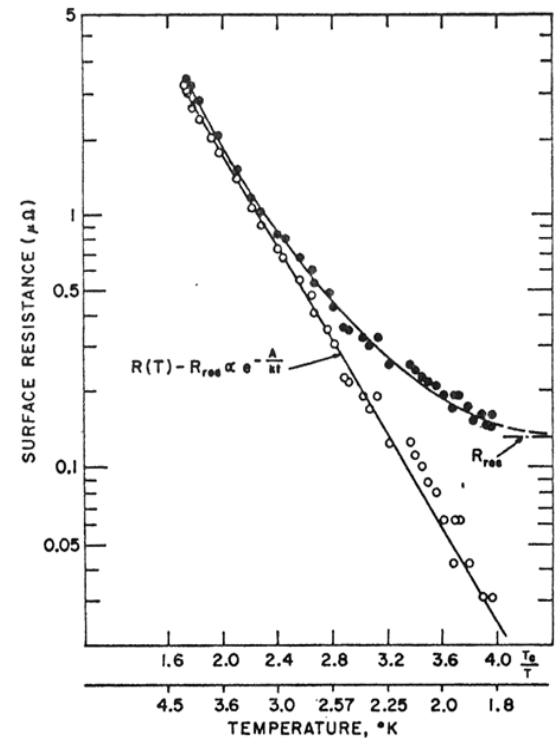
$$R_{BCS}(T, \omega, l) \cong \frac{A(l)\omega^2}{T} e^{-\frac{\Delta}{\kappa_B T}}$$

BCS resistance is caused by electron inertia;

$R_{fl}(B, l) \Rightarrow$  trapped flux surface resistance

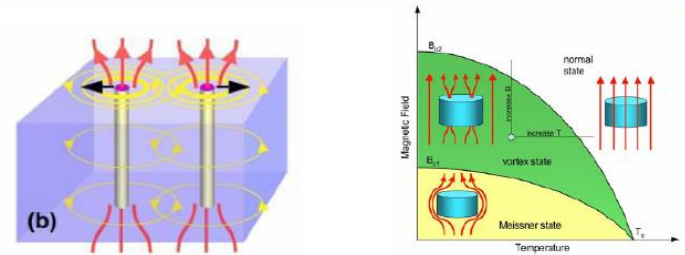
$R_0 \Rightarrow$  intrinsic residual resistance, due to:

- i. Sub-gap states
- ii. Niobium hydrides
- iii. Damaged layer
- iv. ...



J. R. Delayen, SRF1987

**Type-II superconductors**



Main thermodynamic parameters of type-II superconductors:

1. Critical temperature,  $T_c$
2. Lower critical field  $H_{c1}$
3. Upper critical field  $H_{c2}$

# Why SRF?

- For copper cavity at RT ( $\sigma = 5.96e7$  S/m) for  $f=1.3$  GHz one has  $R_s = 9.5$  mOhm.
- For SRF Nb cavity at 2K one has  $R_s = 8.5$  nOhm (ILC –type cavity, electropolishing),

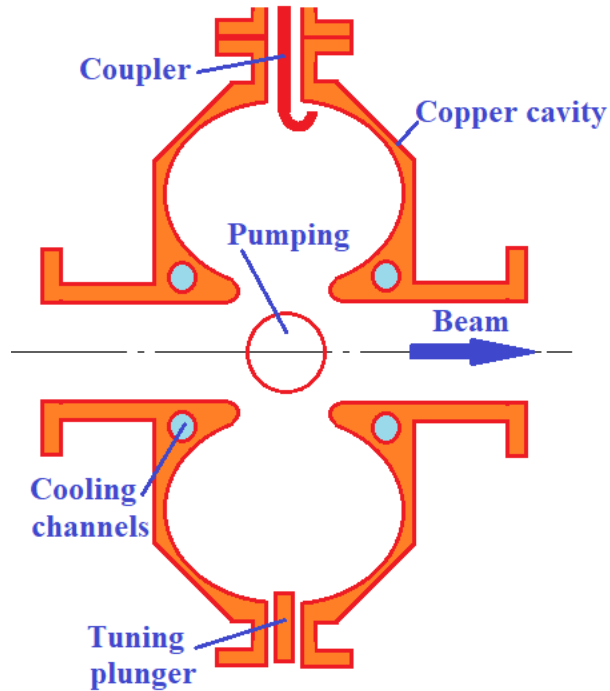
**It is 1.e6 times less!**

Therefore, CW and high Duty Factor are possible at high gradient, even taking into account “conversion factor” for heat removal at 2K (~1000-1200W/W)

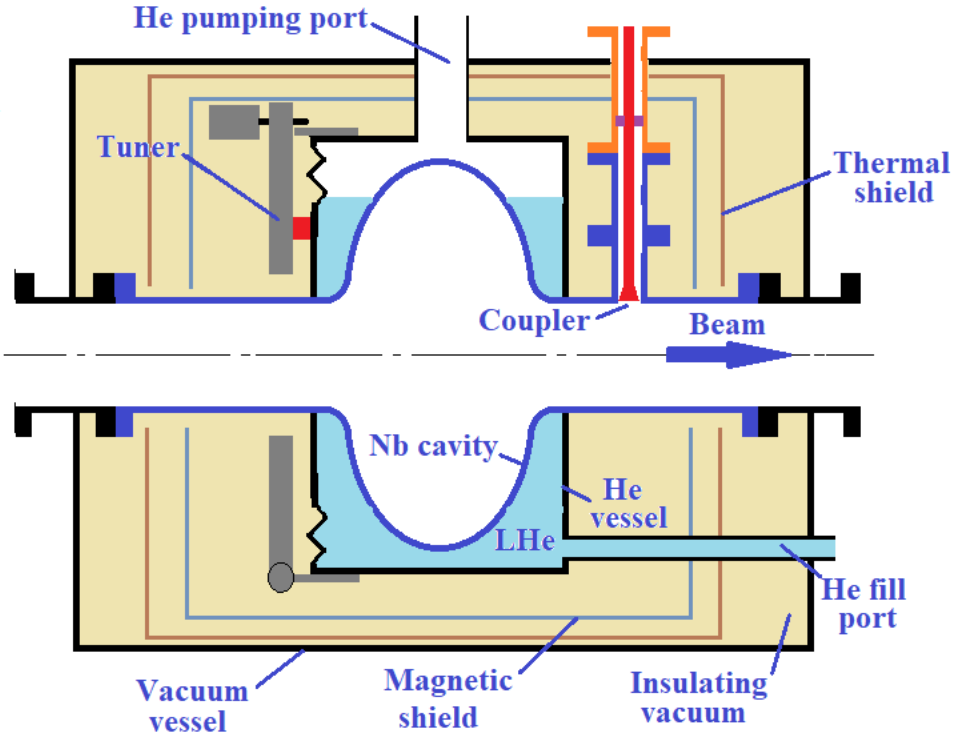


# Why SRF?

RT:  $Q_0 \sim 1e4$



SRF:  $Q_0 \sim 1e10$



## SRF cavity needs:

- Liquid He bath (2K);
- Coarse and fine tuners
- Magnetic shield
- Thermal insulation
- Insulating vacuum
- Cryo plant for liquid He supply

# Why SRF?

## Refrigeration efficiency ( $W_{\text{grid}}/W_{\text{cryo}}$ ):

- Refrigerator's Coefficients of Performance (COP):

$$\text{COP}_{\text{real}} = 1 / (K * \eta_{\text{CARNOT}})$$

$$\eta_{\text{CARNOT}} = T / (300 - T)$$

- Refrigerator's Coefficients of Performance (COP) for different temperatures:

Refrigeration Temperature	Carnot $1/\eta$ IDEAL WORLD	XFEL-Spec REAL WORLD	% Carnot
2 K	149	870	17
5 K	79	220	36
40 K	7	20	33

$$P_{AC} = \sum_T \text{COP}_T \times (P_{\text{dynamic}} + P_{\text{static}})_T$$

**In many cases SRF is more efficient than normal conducting RF!**

- Low and medium beam loading**
- CW and long-pulse operation**

# Why SRF?

**Thus, SC provides the following benefits for electron, ion and proton linacs:**

1. Power consumption is much less

- operating cost savings, better conversion of AC power to beam power
- less RF power sources

2. CW operation at higher gradient possible

- shorter building, capital cost saving
- need fewer cavities for high DF or CW operation
- less beam disruption

3. Freedom to adapt better design for specific accelerator requirements

- large cavity aperture size
- less beam loss, therefore less activation
- HOMs are removed more easily, therefore better beam quality

# Why SRF?

“Practical” gradient limitations for SC cavities:

- Surface magnetic field  $\sim 200$  mT (absolute limit?) – “hard” limit
- Field emission, X-ray, starts at  $\sim 40$  MeV/m surface field – “soft” limit
- Thermal breakdown (limits max surface field for  $f > 2$  GHz for typical thickness of material, can be relaxed for thinner niobium) - “hard” limit

SRF allows significantly higher acceleration gradient than RT at high Duty Factor and CW!

# Why SRF?

Different mechanisms limiting acceleration gradient:

Room Temperature:

- *Vacuum Breakdown;*
- *Metal fatigue caused by pulse heating;*
- *Cooling problems.*

Breakdown limit:

$$E_a \cdot t_p^{1/6} = \text{const}$$

$E_a \sim 20 \text{ MV/m}$  ( $E_{pk} \sim 40 \text{ MV/m}$ ) @ 1ms or

$E_a \sim 7 \text{ MV/m}$  ( $E_{pk} \sim 14 \text{ MV/m}$ ) @ 1sec (CW)

Superconducting:

- Breakdown usually is not considered for SC cavity;
- Thermal breakdown (quench) – for >2 GHz

# Why SRF?

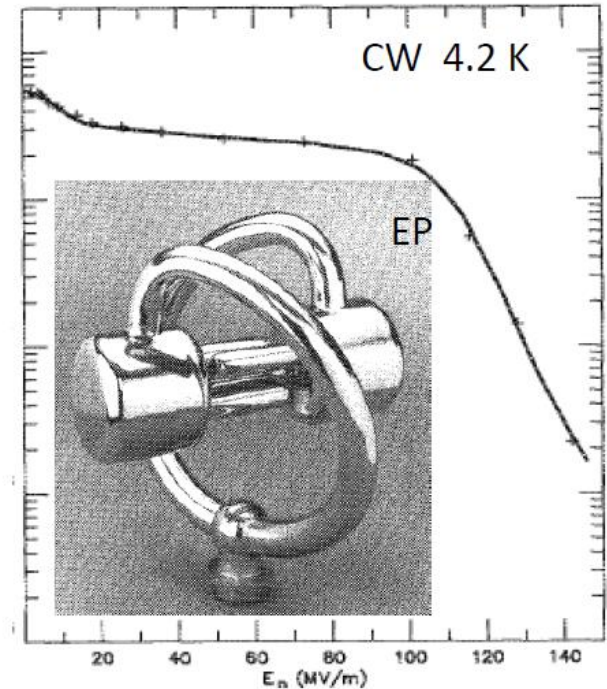
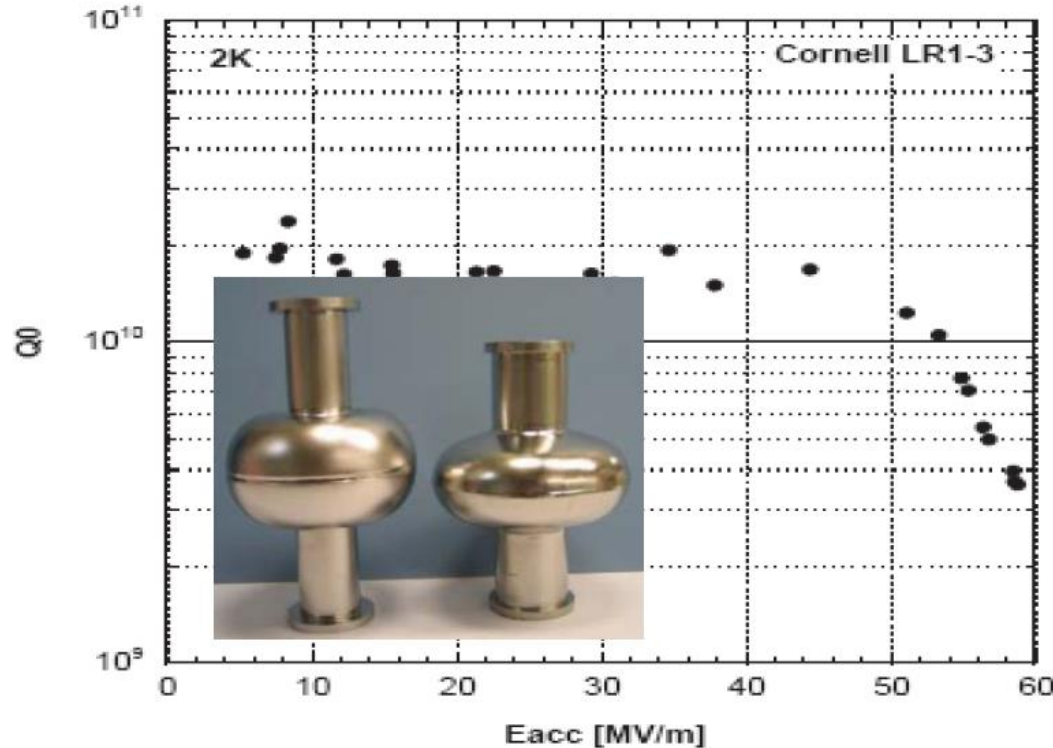
## Achieved Limit of SRF electric field

- No known theoretical limit
- 1990: Peak surface field  $\sim 130$  MV/m in CW and 210 MV/m in 1ms pulse.

*J. Delayen, K. Shepard, "Test a SC rf quadrupole device", Appl. Phys. Lett, 57 (1990)*

- 2007: Re-entrant cavity:  $E_{\text{acc}} = 59$  MV/m ( $E_{\text{pk}} = 125$  MV/m,  $B_{\text{pk}} = 206.5$  mT).

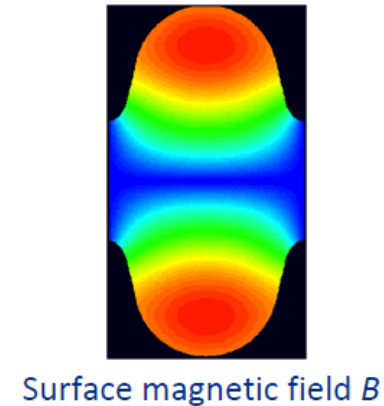
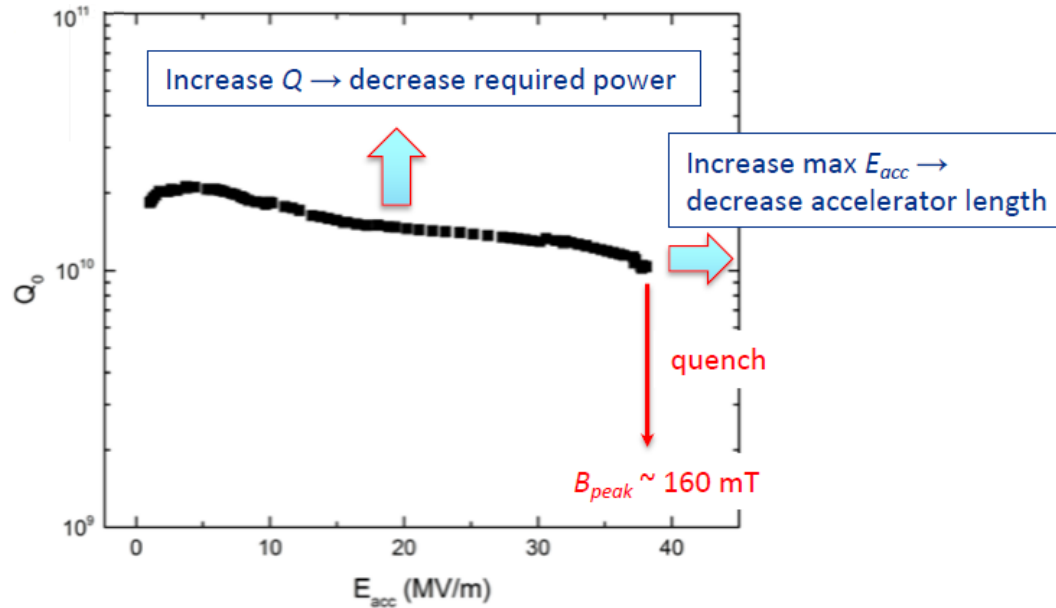
*(R.L. Geng et. al., PAC07\_WEPMS006) – World record in accelerating gradient*



# Why SRF?

## Introducing $Q_0$ vs. $E_{acc}$ plot:

*Typical ILC-prepared TESLA cavity at  $T = 2$  K (state of the art until recent breakthroughs)*



- It is customary to represent performance of an SRF cavity using  $Q_0$  vs.  $E_{acc}$  or  $Q_0(E_{acc})$  plot.
- Peak surface electric and magnetic fields in the cavity are proportional to  $E_{acc}$ . Sometimes  $Q_0$  is plotted vs. peak fields.



# Why SRF?

## SC cavity performance limitations

▪ Ideal performance:  $Q_0$  is constant until the maximal surface magnetic field is reached:

→ fundamental limitation, limits accelerating gradient to  $\sim 60$  MV/m for typical Nb elliptical cavity shapes.

▪ **Why is  $Q_0(E_{acc})$  different in real life?**

Here are some limitations that historically plagued the SRF cavity performance:

- High surface electric field → field emission

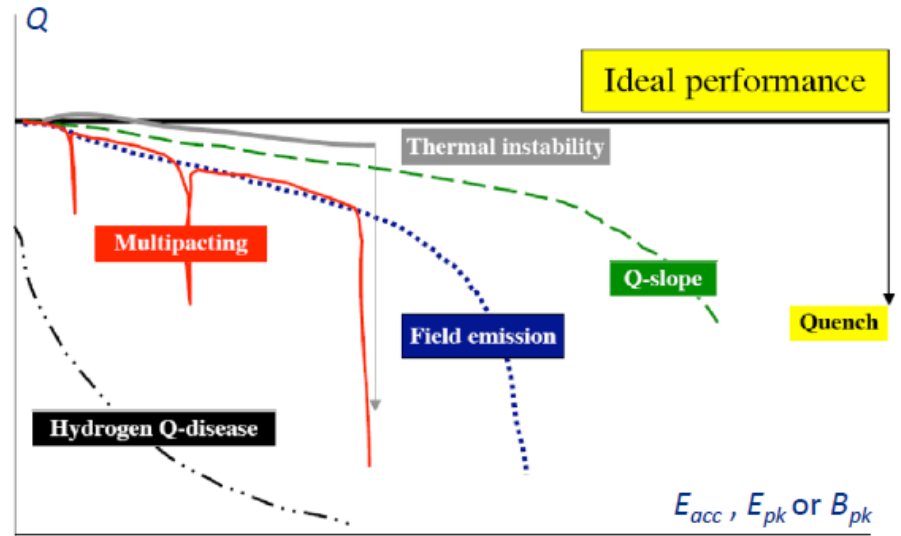
→ can be cured by applying proper preparation techniques: clean room (particulate-free) assembly, high-pressure DI water rinsing (HPR), mechanical polishing of the inner cavity surface.

- Thermal quench → use of high-purity material (RRR) to improve thermal conductivity\*, material quality control to avoid mechanically damaged surfaces, particulate free assembly.

- Multipacting → use of elliptical cell shapes.

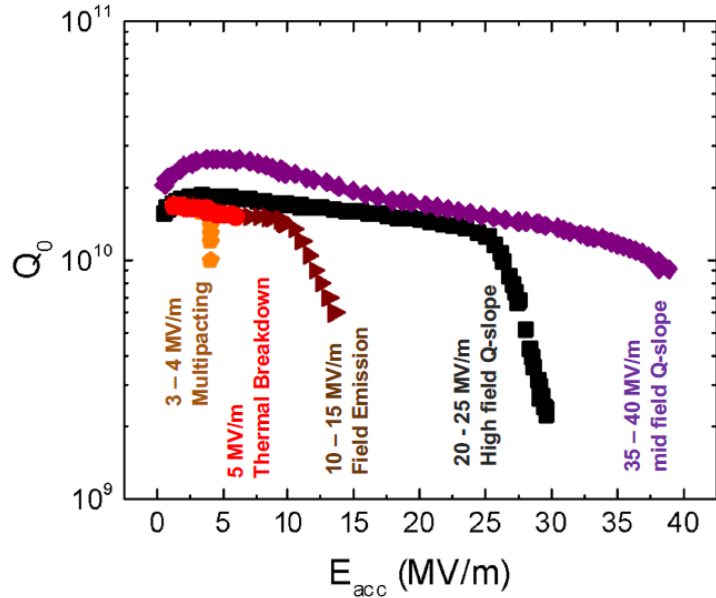
Q-disease due to lossy niobium hydrides → perform acid etch at  $T < 15^\circ\text{C}$ , rapid cooldown, degassing at  $600 - 800^\circ\text{C}$ .

\***Wiedemann–Franz law** states that the ratio of the electronic contribution of the thermal conductivity ( $\kappa$ ) to the electrical conductivity ( $\sigma$ ) of a metal is proportional to the temperature ( $T$ ), or  $\kappa = \sigma LT$ ,  $L$  is Lorentz number.

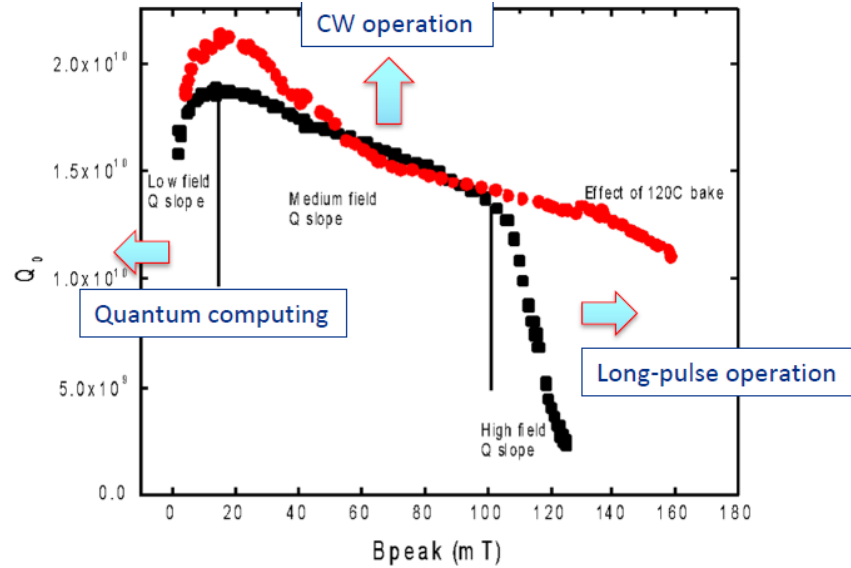


# Why SRF?

## $Q_0(E_{acc})$ with numbers



## Q slopes



Three parts of the curve limiting performance of different applications:

1. Low field Q slope → SRF for quantum computing: need as high Q as possible to increase qubit coherence time;
2. Medium field Q slope → CW operation: cryogenics vs. linac cost optimization determines operating gradient (15-20 MV/m, LCLS-II);
3. High field Q slope → Long-pulse operation tends to favor the highest reliably achievable gradient (23.6 MV/m for XFEL, 31.5 MV/m for ILC)

# Why SRF?

## Standard SRF cavity surface treatments

### Electron-Beam Welding - EBW

### Buffered Chemical Polishing –BCP: $\text{HNO}_3 + \text{HF} + \text{H}_3\text{PO}_4$

- $\text{H}_3\text{PO}_4$  (phosphoric acid) is necessary to stabilize (buffer) the etching reaction between Nb and  $\text{HNO}_3$  (nitric acid) + HF (hydrofluoric acid), which is exothermic and rapid.
- The mixture is used for Nb cavities contains HF(48%),  $\text{HNO}_3$  (65%),  $\text{H}_3\text{PO}_4$ (98%) in proportion 1:1:X, X=1-4.
- Still in use for low-frequency, medium gradient cavities;

### Electro-Polishing –EP: $\text{H}_2\text{SO}_4 + \text{HF} + 10\text{-}12\text{V} \rightarrow$ smooth surface, lower surface fields, lower FE, higher $E_{\text{acc}}$ and $Q_0$ .

- A cathode made of pure Al and a Nb cavity as an anode in mixture of sulfuric acid  $\text{H}_2\text{SO}_4$  (93%) and hydrofluoric acid HF (50%) at 10:1 volume ratio.
- Nb is oxidized by sulfuric acid to niobium-pentoxide, which is dissolves simultaneously by hydrofluoric acid.
- Used for high-gradient cavities in pulsed regime and for medium-gradient cavities in CW.

### High-Temperature Treatment

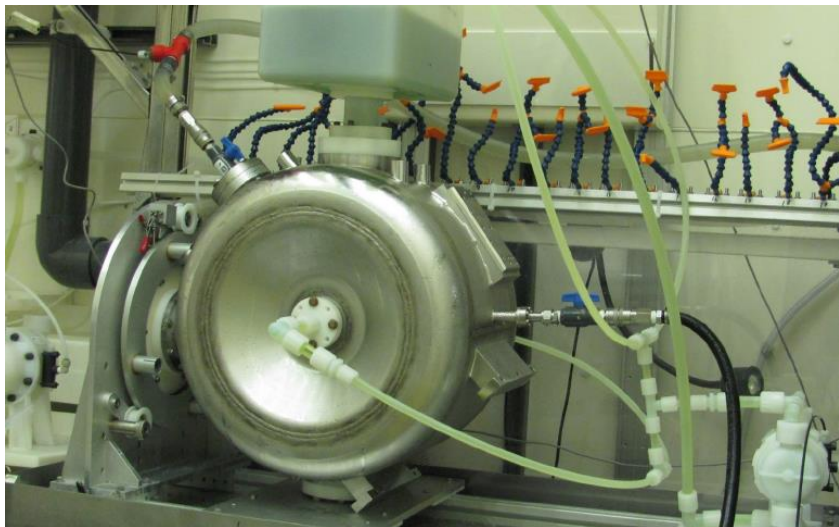
- 800C -900C backing in vacuum is used to relieve the stresses, remove defects and dislocations and degas of hydrogen.

### High-Pressure Rinsing (HPR)

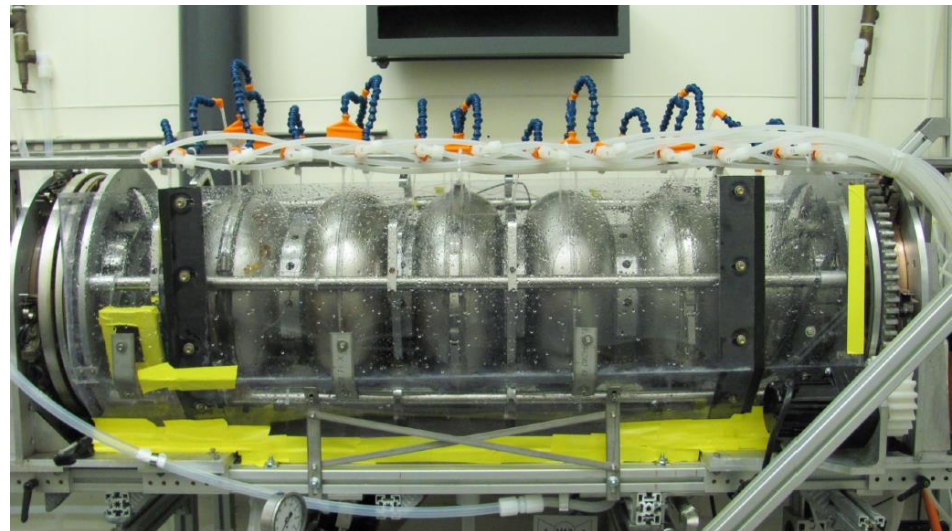
- 100 bar rinsing before assembly in a clean room

# Why SRF?

BCP processing for a 325 MHz spoke cavity.



EP processing of 650 MHz elliptical cavity



# Why SRF?

- $Q_0$  Improvement:
  - Improvement of cavity processing recipes;
  - High  $Q_0$  preservation in CM.
- The goal is to achieve  $Q_0 > 2.5e10 - 4e10$  in CM

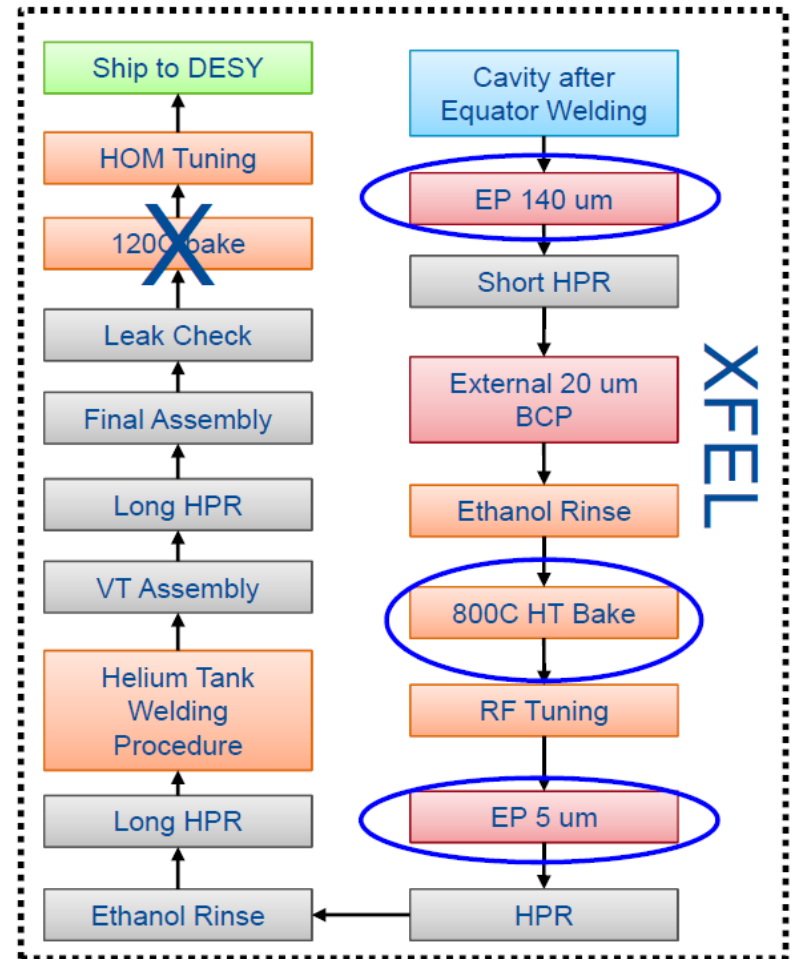
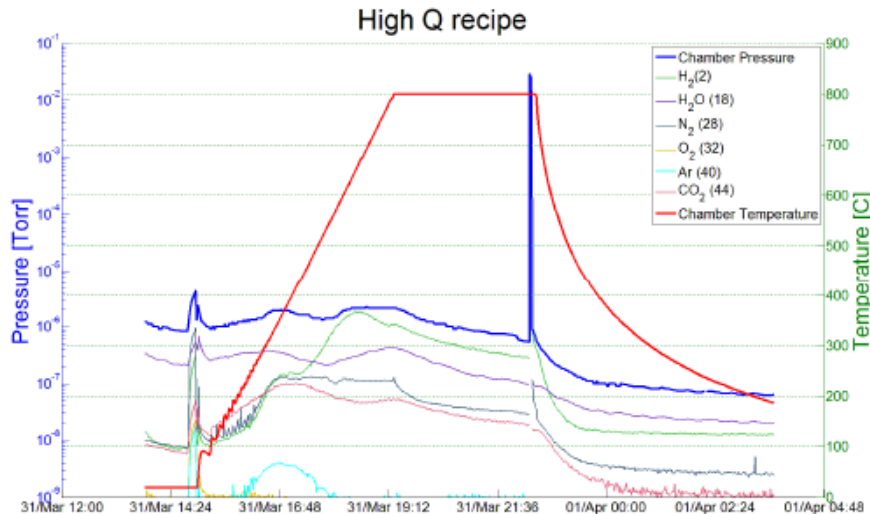


# Recent breakthrough in $Q_0$ increase: N-doping.

- “Standard” XFEL technology provides  $\sim 1.4e10 @ 2K$ , 20-23 MeV/m (CM);
- N-doping: discovered in the frame of R&D on the Project-X SC CW linac (A. Grassellino).

Cavity Treatment:

- Bulk EP
- 800 C anneal for 3 hours in vacuum
- 2 minutes @ 800C nitrogen diffusion
- 800 C for 6 minutes in vacuum
- Vacuum cooling
- 5 microns EP

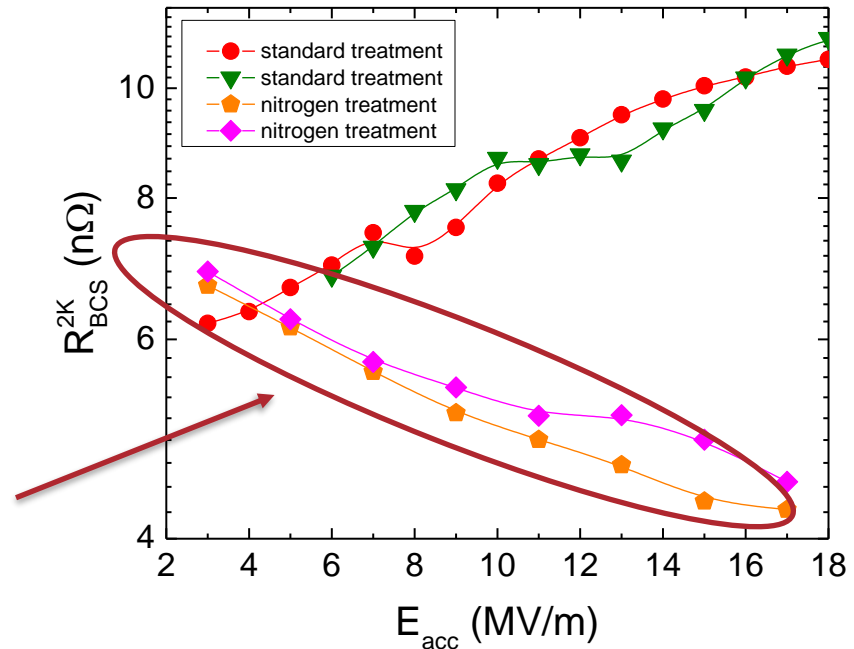
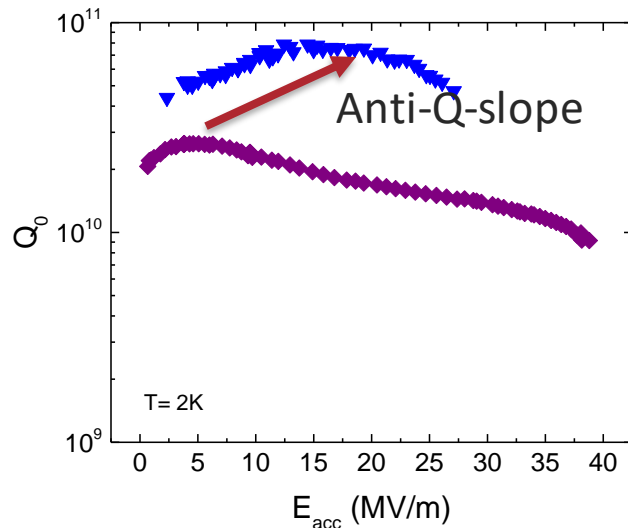


A. Grassellino, N-doping: progress in development and understanding, SRF15

# N-doping

## Origin of the anti-Q-slope for N-doping

$$R_S(2 K) = R_{BCS}(2 K) + R_0 + R_{fl}$$



Anti-Q-slope emerges from the BCS surface resistance decreasing with field

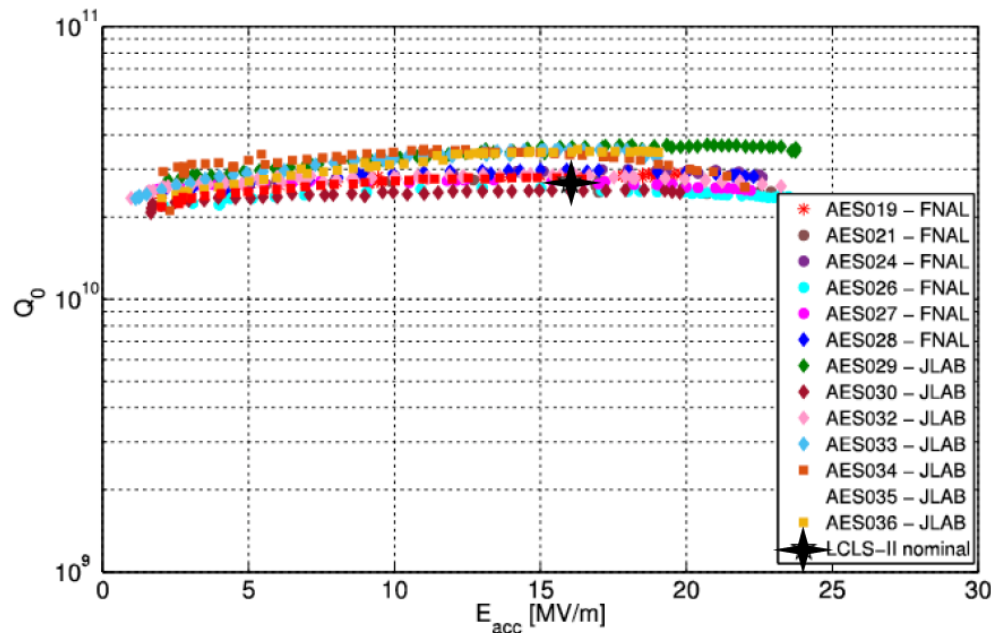
A. Grassellino et al, Supercond. Sci. Technol. **26** 102001 (2013) - Rapid Communications  
A. Romanenko and A. Grassellino, Appl. Phys. Lett. **102**, 252603 (2013)

M. Martinello, M. Checchin



# N-doping:

- Provides  $Q_0$  2.5-3 times higher than “standard” processing.
- Trade-off:
  - Lower acceleration gradient, 20-22 MeV/m – not an issue for ion and proton linacs;
  - Higher sensitivity to the residual magnetic field.
- Remedy:
  - Magnetic hygiene and shielding improvement
  - Fast cooldown

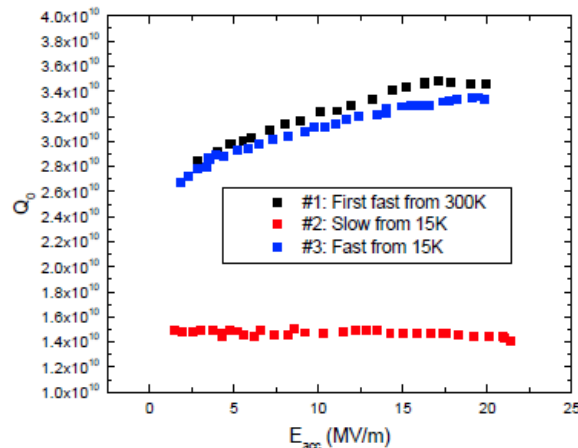


VTS test results of dressed prototype cavities

# Fast cooldown

- $Q_0 = G/R_s$ ;  $R_s = 10$  nOhm for  $Q_0 = 2.7e10$   
 $R_s = R_0 + R_{BCS} + R_{TF}$ ,  
 $R_{TF} = s * \eta * B_{res}$ ,  $s$  is sensitivity to residual magnetic field  $B_{res}$ ,  $\eta$  is flux expulsion efficiency.  
 **$\eta$  is material-dependent!**
- For pCM Nb (Wah Chang):  
 $R_{BCS} = 4.5$  nOhm,  $R_0 = 1-2$  nOhm,  $R_{TF} \approx 1$  Ohm for 5mG  $\rightarrow Q_0 = 3.5e10$
- For production material:  
Change heat treatment temperature from 800 C to 900 C+ deeper EP (S. Posen):  
 $R_{BCS} = 4.5$  nOhm,  $R_0 \approx 2$  nOhm,  $R_{TF} \approx 2$  Ohm for  $B_{res} \approx 5$ mG  $\rightarrow Q_0 > 3e10$

Dressed N<sub>2</sub> doped 9 cell Sensitivity Test at 2K

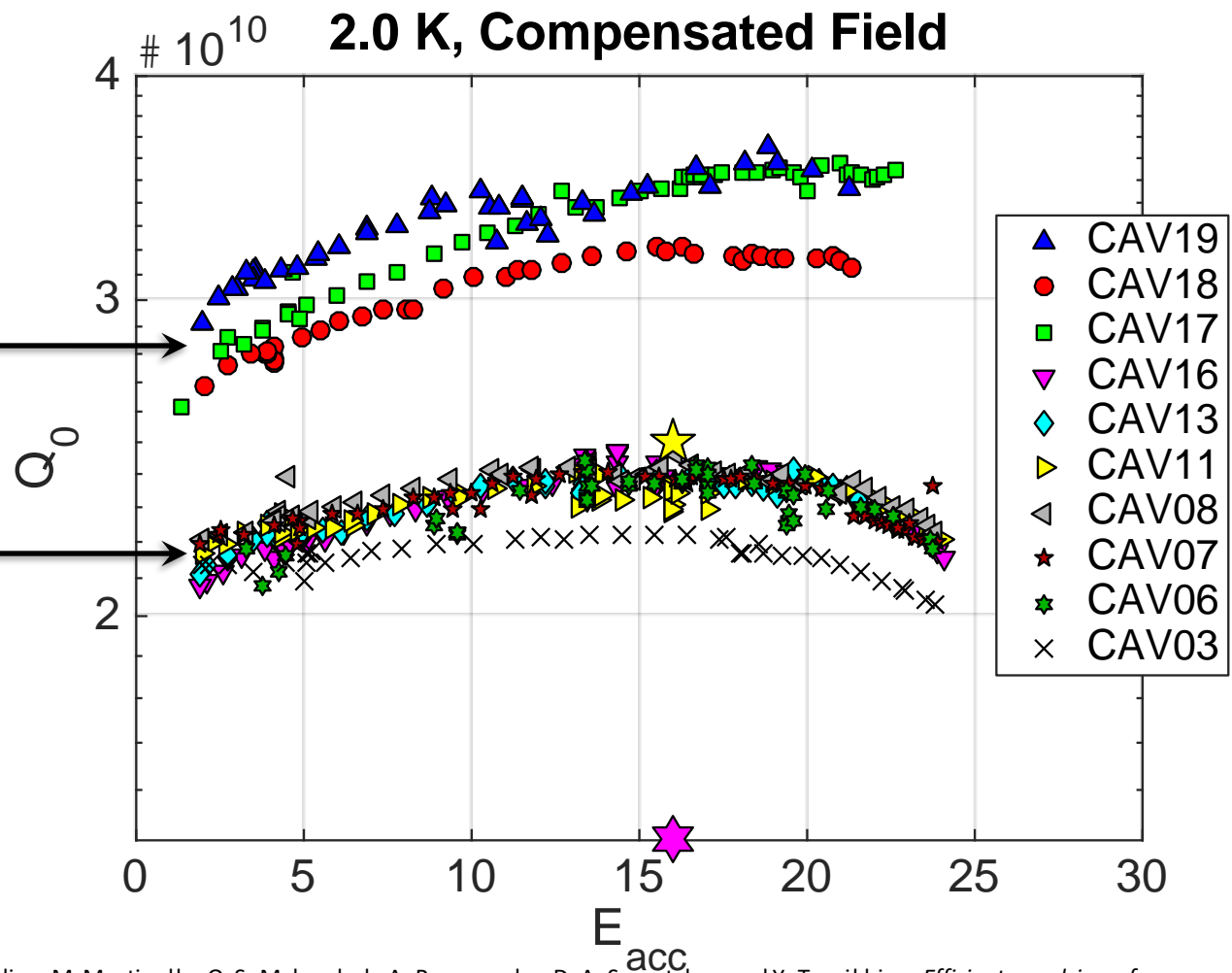


“Fast”: 2 – 3 K/minute , “slow”: < 0.5 K/minute

# Impact of Modified LCLS-II Recipe on $Q_0$

**Cavities 17, 18, 19:**  
modified recipe - 900 C degas,  $\sim 200 \mu\text{m}$  EP, 2min/6min N doping at 800 C

**Cavities 03...16:** First production tests at Fermilab, baseline LCLS-II recipe - 800 C degas,  $\sim 130 \mu\text{m}$  EP, 2min/6min N doping at 800 C



Studies leading to modified recipe:

S. Posen, M. Checchin, A. C. Crawford, A. Grassellino, M. Martinello, O.S. Melnychuk, A. Romanenko, D. A. Sergatskov and Y. Trenikhina, *Efficient expulsion of magnetic flux in superconducting radiofrequency cavities for high  $Q_0$  applications*, J. Appl. Phys. **119**, 213903 (2016), [dx.doi.org/10.1063/1.4953087](https://doi.org/10.1063/1.4953087).

A. Romanenko, A. Grassellino, A. C. Crawford, D. A. Sergatskov and O. Melnychuk, *Ultra-high quality factors in superconducting niobium cavities in ambient magnetic fields up to 190 mG*, Appl. Phys. Lett. **105**, 234103 (2014); [http://dx.doi.org/10.1063/1.4903808](https://doi.org/10.1063/1.4903808).

A. Grassellino, A. Romanenko, S Posen, Y. Trenikhina, O. Melnychuk, D.A. Sergatskov, M. Merio, N-doping: progress in development and understanding, Proceedings of SRF15, <http://srf2015proc.triumf.ca/prepress/papers/moba06.pdf>.

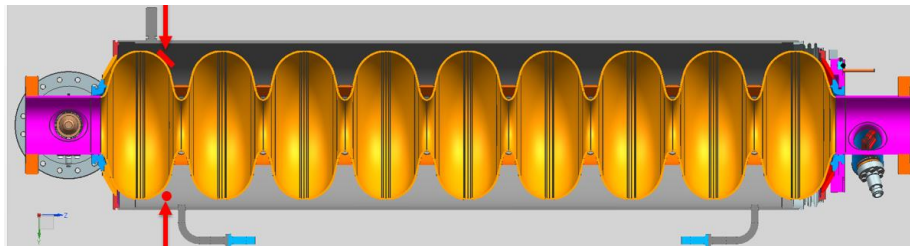


# Ambient Magnetic Field Management Methods

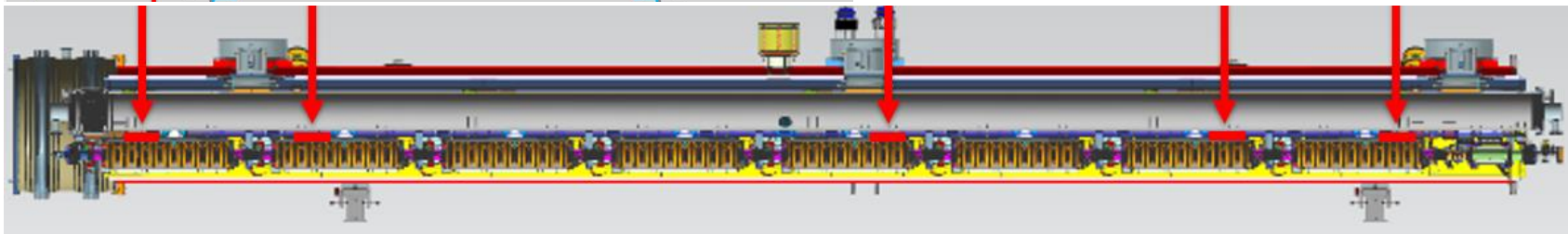
- 2-layer passive magnetic shielding
  - Manufactured from Cryoperm 10
- Strict magnetic hygiene program
  - Material choices
  - Inspection & demagnetization of components near cavities
  - Demagnetization of vacuum vessel
  - Demagnetization of assembled cryomodule / vessel
- Active longitudinal magnetic field cancellation

## Magnetic field diagnostics:

- 4 cavities instrumented with fluxgates inside helium vessel (2 fluxgates/cavity)
- 5 fluxgates outside the cavities mounted between the two layers of magnetic shields



Fluxgates monitored during cryomodule assembly

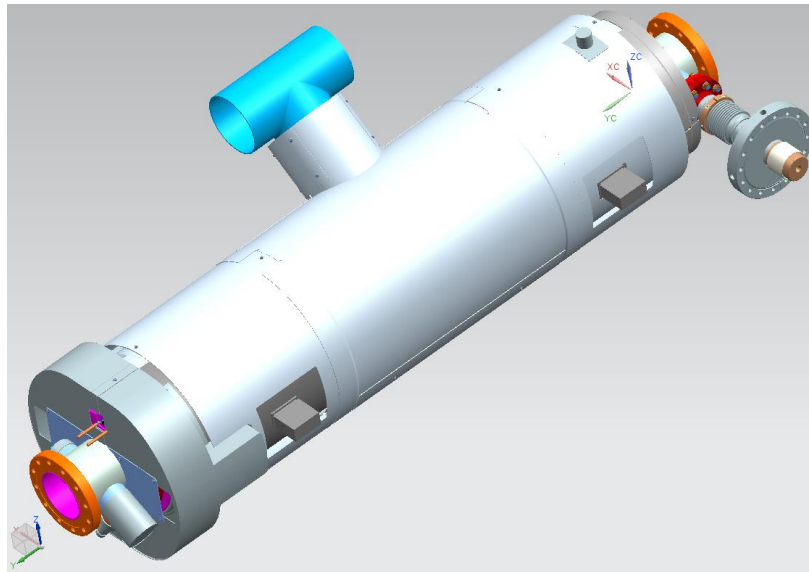


A. Crawford, arXiv:1507.06582v1, July 2015; S. Chandrasekaran, TTC Meeting, Saclay 2016

# Ambient Magnetic Field Management Methods

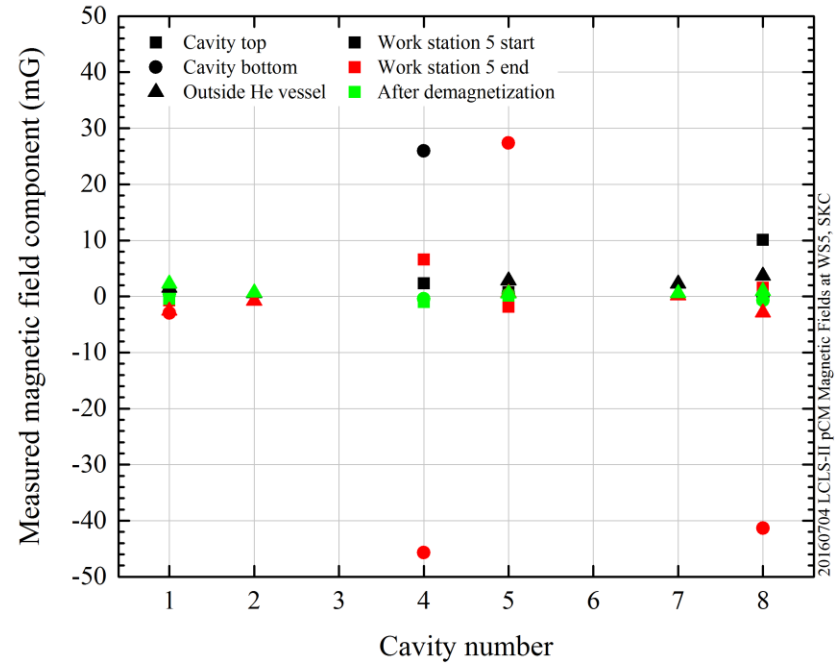


Helmholtz coils wound onto vessel directly



2-layer magnetic shields  
manufactured from Cryoperm 10

S. Chandrasekaran, Linac 2016, TUPLR027



# Prototype Cryomodule Latest Preliminary Results

- Cryomodule remnant field  $\approx 1$  mG
- Fast cool down in a cryomodule demonstrated
- $Q_0 \approx 2.7e10$  in a CW cryomodule

Cavity	VTS		pCM after RF_Conditioning			
	Max Gradient [MV/m]	$Q_0$ @16MV/m	Max Gradient*** [MV/m]	Usable Gradient* [MV/m]	FE onset [MV/m]	$Q_0$ @16MV/m 2K** extrapolated
TB9AES021	23	3.1E+10	19.6	18.2	14.6	2.6E+10
TB9AES019	19.5	2.8E+10	19	18.8	15.6	2.6E+10
TB9AES026	21.4	2.6E+10	17.3	17.2	17.4	2.7E+10
TB9AES024	22.4	3.0E+10	21	20.5	21	2.5E+10
TB9AES028	28.4	2.8E+10	14.9	14.2	13.9	2.4E+10
TB9AES016	18	2.8E+10	17.1	16.9	14.5	2.9E+10
TB9AES022	21.2	2.8E+10	20	19.4	12.7	3.2E+10
TB9AES027	22.5	2.8E+10	20	17.5	20	2.5E+10
<b>Average</b>	<b>22.1</b>	<b>2.8E+10</b>	<b>18.6</b>	<b>17.8</b>	<b>16.2</b>	<b>2.7E+10</b>
<b>Total Voltage</b>	<b>183.1 MV</b>		<b>154.6</b>	<b>148.1</b>		

\*Usable Gradient: demonstrated to stably run CW, FE < 50 mR/h, no dark current

\*\*Fast cooldown from 45K, >40 g/sec, extrapolated from 2.11K

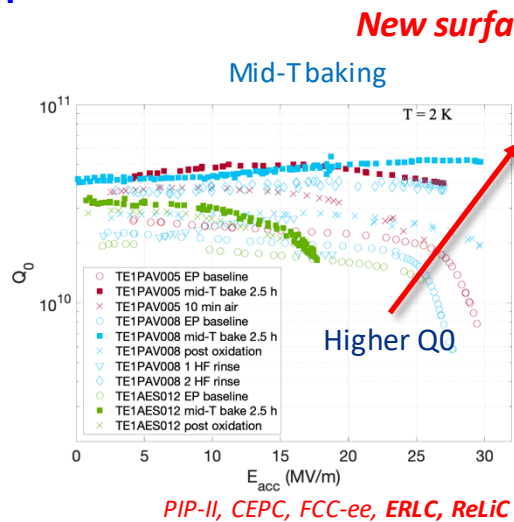
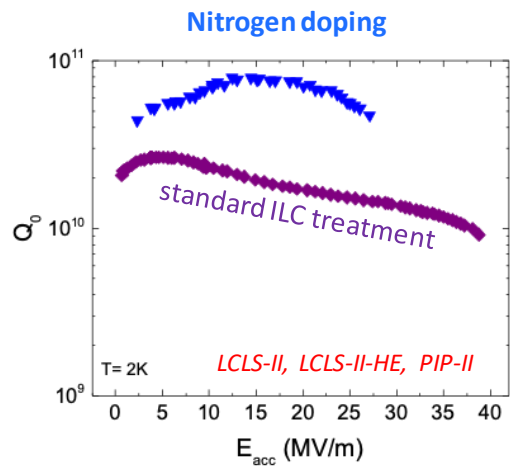
G. Wu, FNAL SRF Department meeting, 24 October 2016, <https://indico.fnal.gov/conferenceDisplay.py?confId=13185>



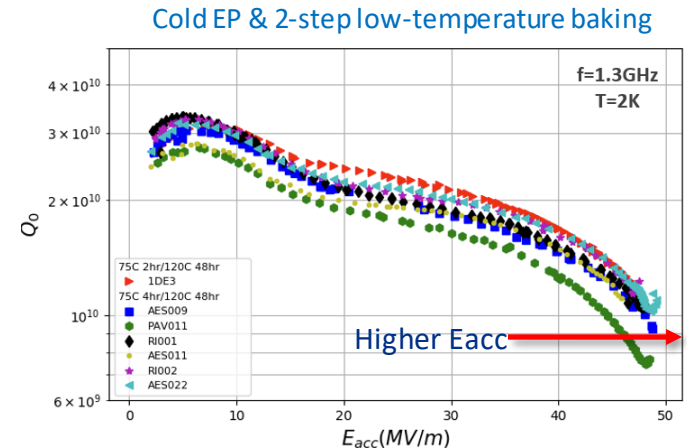


# Further Improving cavity performance via surface treatment

- Breakthrough caused by invention of **nitrogen doping** (N-doping) triggered investigations of other surface treatment methods:
  - Mid-T backing and
  - Cold EP & 2-step baking.



## New surface treatments



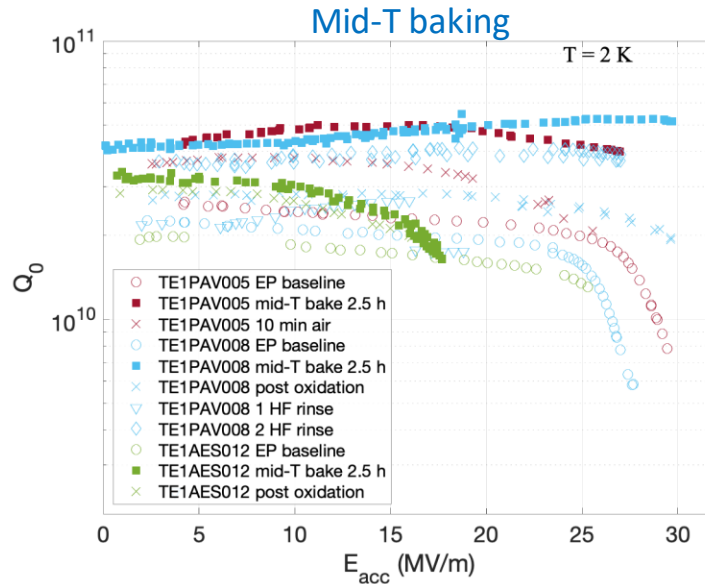
ILC, HELEN, 8-GeV linac at FNAL

- There are active studies to push performance of bulk niobium cavities, improve our understanding of SRF losses and ultimate quench fields via experimental and theoretical investigations
- The ultimate goal is on developing methods for nano-engineering the niobium surface layer and tailoring SRF cavity performance to a specific application

## Mid-T baking: Initial results

- Medium temperature baking in vacuum (Mid-T, 300°C to 400°C) was developed to improve cryogenic performance of SRF cavities at medium accelerating gradients ( $E_{acc} = 20 - 30$  MV/m), extending beyond N-doping in  $E_{acc}$  while maintaining high  $Q_0$

This is a new, simpler alternative to nitrogen doping



S. Posen et al. *Phys. Rev. Applied* **13**, 014024 (2020)

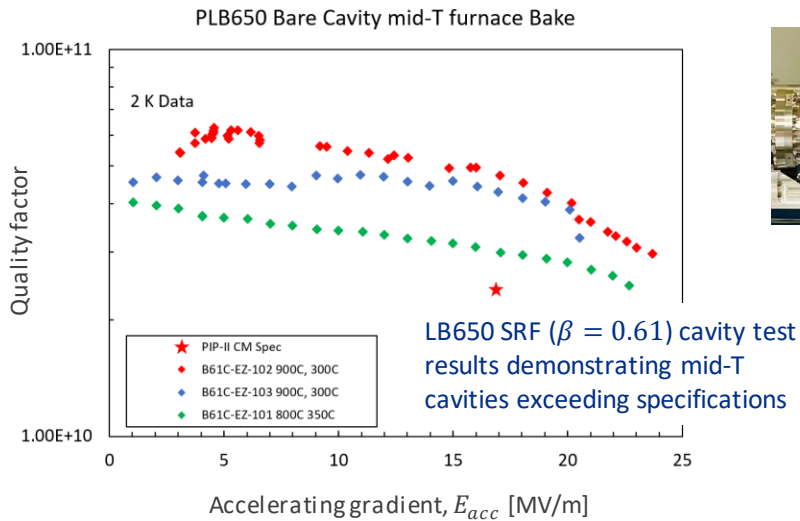


**Note:** Our standard “vehicle” for R&D is a single-cell 1.3 GHz elliptical TESLA shape cavity

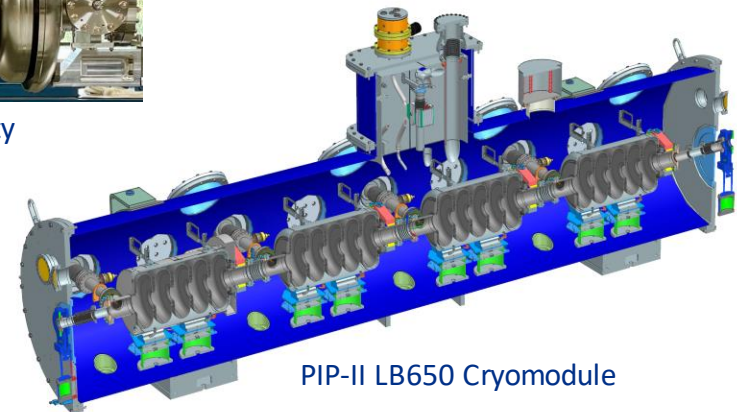


## Mid-T baking at 650 MHz (5-cell cavities)

- After initial R&D efforts at 1.3 GHz, this recipe was successfully tested on the low-beta 650 MHz (LB650) PIP-II cavities and was accepted as a baseline treatment



PIP-II LB650 SRF cavity



PIP-II LB650 Cryomodule

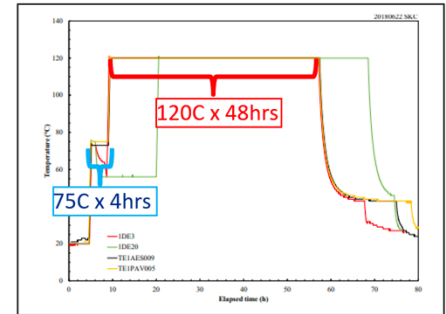
Courtesy of Genfa Wu (FNAL)

**Note:** Need to multiply  $Q$  by a factor of 1.4 to compare with TESLA shape cavities

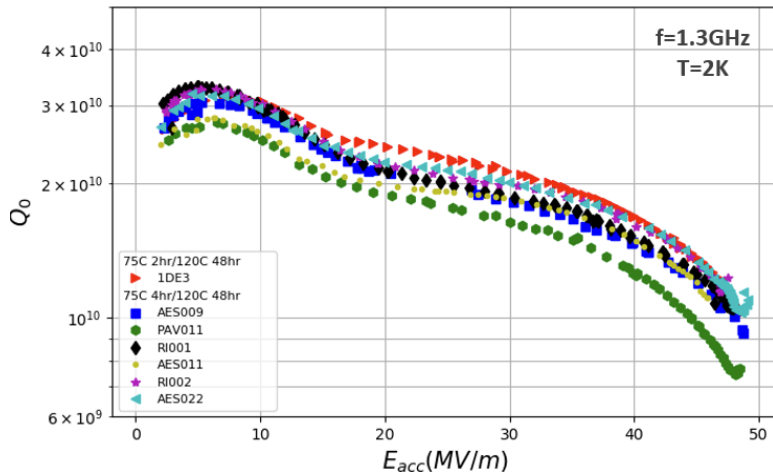
- Mid-T baking is relevant to ERL-based liner colliders (as well as circular colliders)

# Pushing toward 50 MV/m

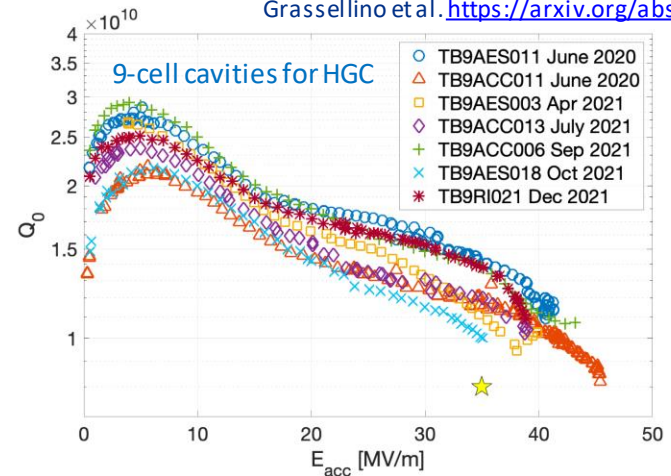
- Application of a combination of cold electropolishing (EP) and 2-step low-temperature baking to single-cell TESLA cavities demonstrated accelerating gradients  $\sim 50$  MV/m
- The recipe is transferred to 9-cell cavities: average 40.4 MV/m!
- A High-Gradient Cryomodule (HGC) is being prepared at Fermilab for testing



2-step low-temperature baking (single-cell cavities)

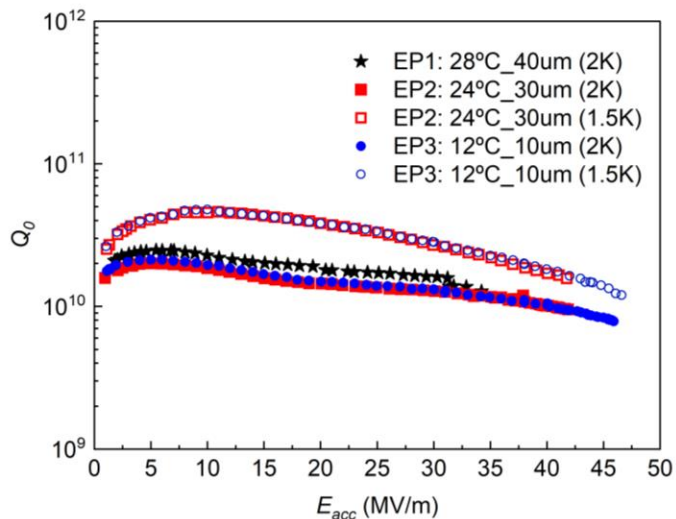


Grassellino et al. <https://arxiv.org/abs/1806.09824>

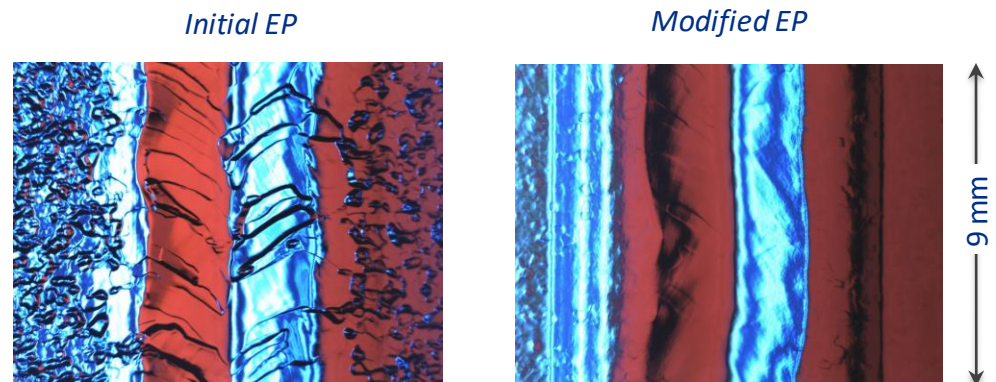


## Cold EP or 2-step baking?

- It is not clear yet, whether cold EP, 2-step baking (as opposed to standard low-temperature baking) or a combination of both is responsible for improving accelerating gradient
- Cold EP provides much smoother surface than EP at higher temperatures
- Recently, a 9-cell cavity subjected to cold EP and 120°C baking reached 46 MV/m
- Systematic studies are under way



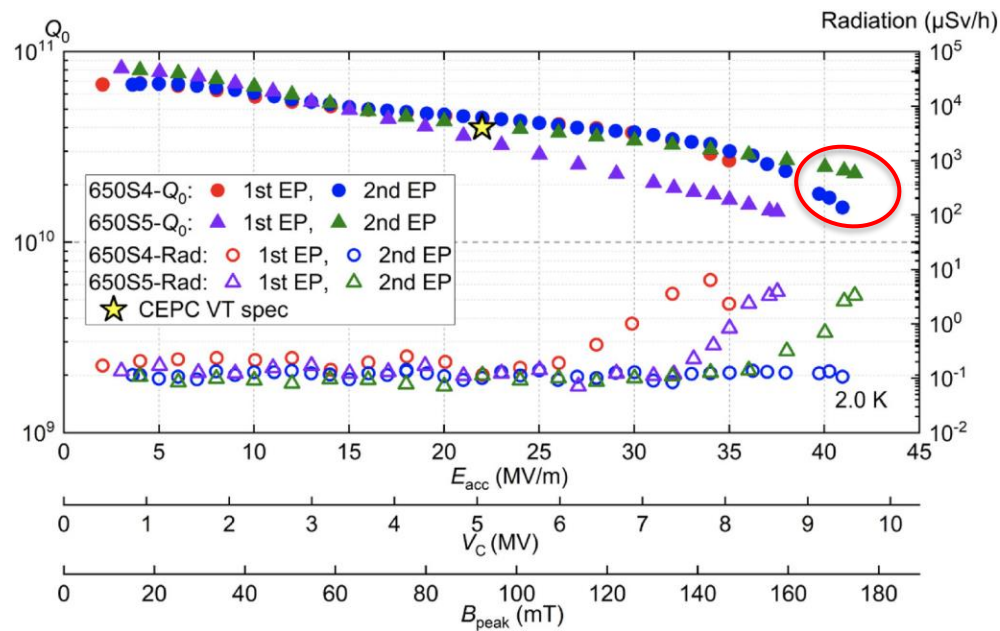
Courtesy of V. Chouhan (FNAL)



V. Chouhan *et al.*, *Nucl. Instrum. Methods Phys. Res. A* **1051** (2023) 168234

# Recent results on single-cell 650 MHz cavities

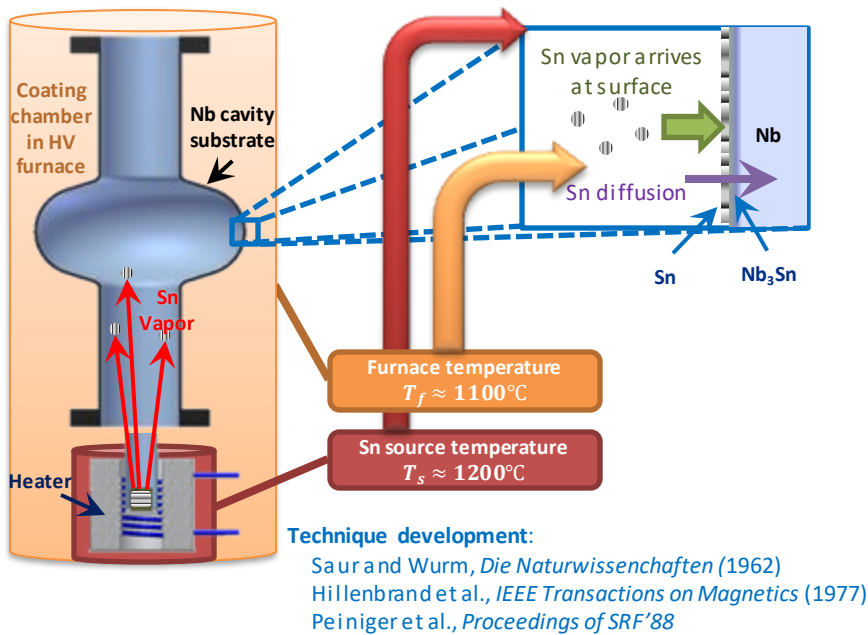
- Recently, cold EP and 120°C backing applied to single-cell 650 MHz cavities produced excellent results at IHEP (China)
- Similar performance was demonstrated at Fermilab



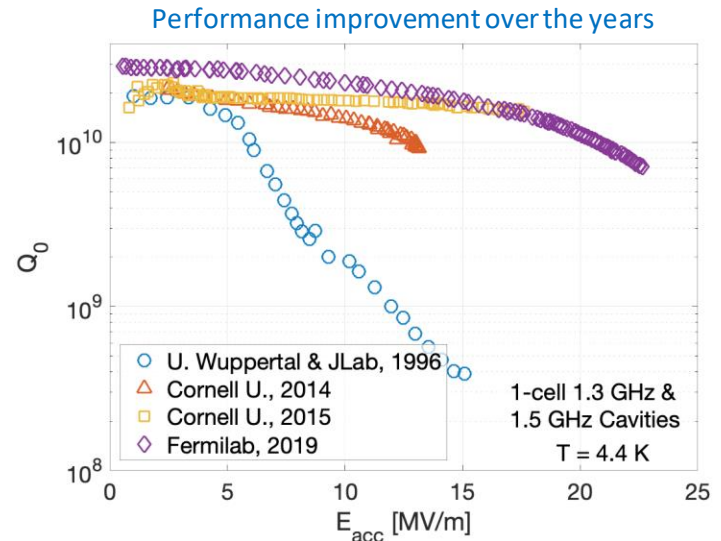
P. Sha et al. *Nucl. Sci. Tech.* (2022) **33**:125

# New materials: Nb<sub>3</sub>Sn

- High  $T_c$  material → low losses at 4 K, a candidate for cryocooler-based applications
- Potential for high gradients, ~ 90 MV/m**
- So far, the best progress with **vapor diffusion technique**

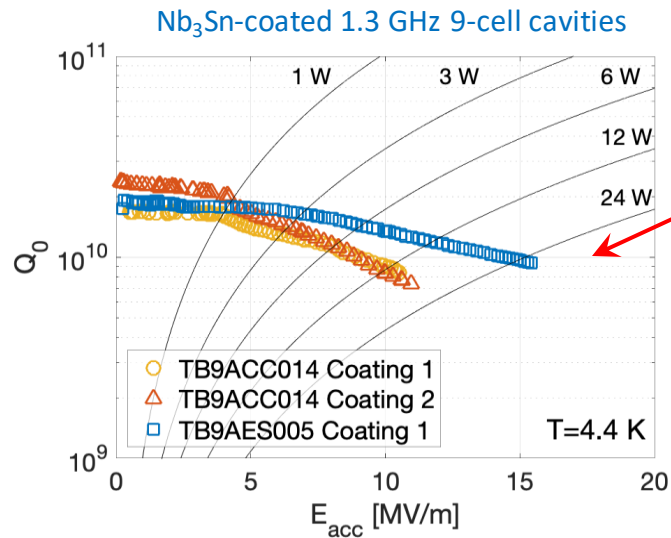


- Best performance of a single-cell Nb<sub>3</sub>Sn cavity so far is only ~ 24 MV/m

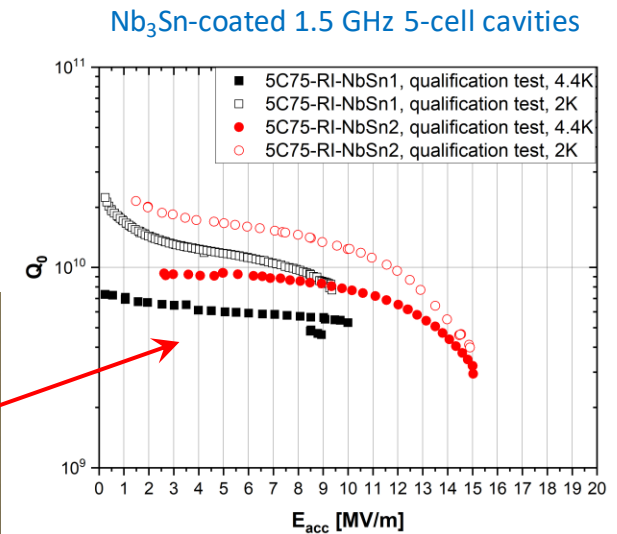
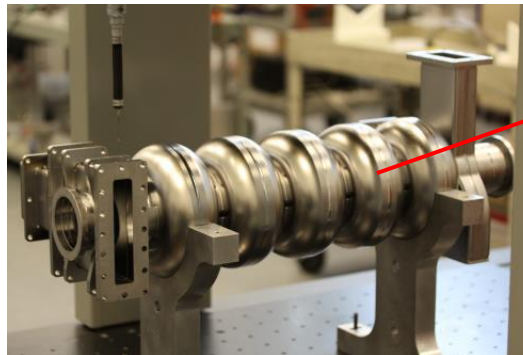
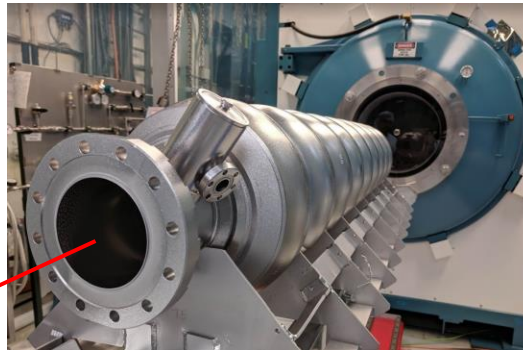


# Multi-cell Nb<sub>3</sub>Sn cavities

- The best multi-cell cavities reached 15 MV/m



Courtesy of S. Posen (FNAL)



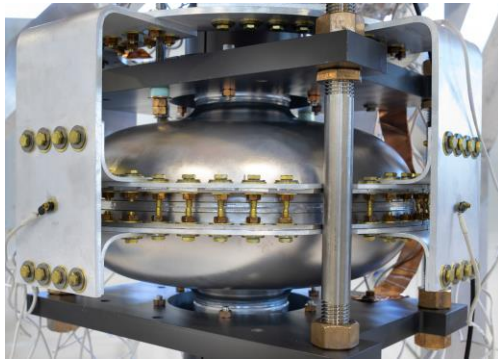
G. Ereemeev and U. Pudasaini, presentation at the *TTC meeting*, October 2022



# Conduction-cooled cavities

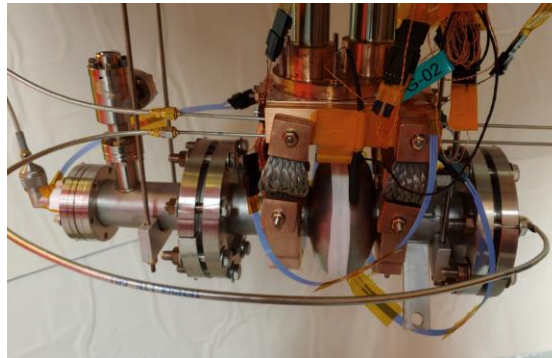
- Conduction cooling of Nb<sub>3</sub>Sn SRF cavities via a cryocooler was demonstrated recently
- This is promising for **new compact accelerator applications for industry**

Fermilab



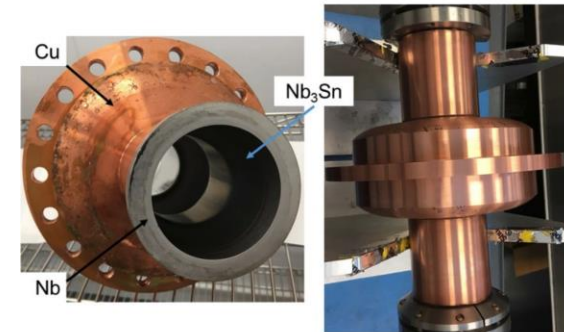
R.C. Dhuley et al, *Supercond. Sci. Technol.* **33**, 06LT01 (2020)

Cornell University



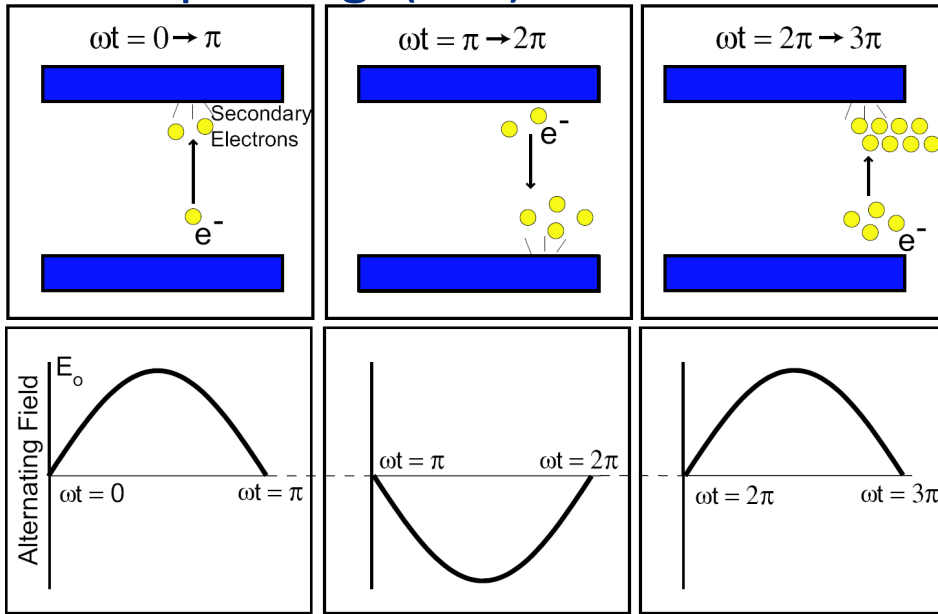
N. Stilin et al, arXiv:2002.11755v1 (2020)

Jefferson Lab

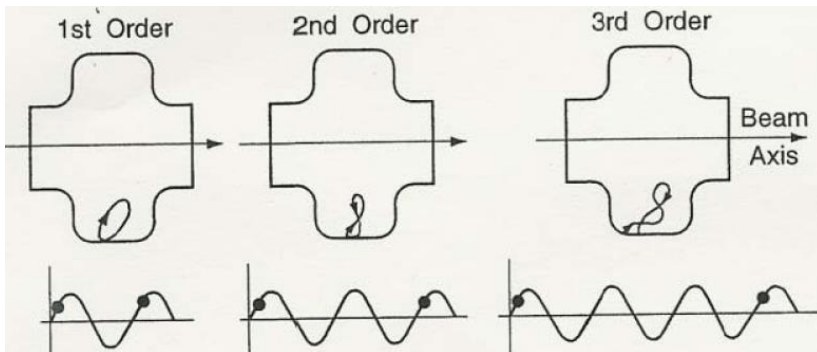


G. Ciovati et al, *Supercond. Sci. Technol.* **33**, 07LT01 (2020)

# Multipacting (MP) in SRF cavities

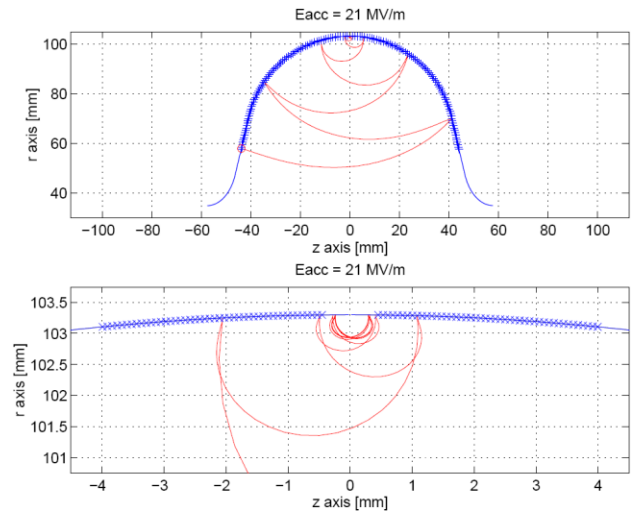
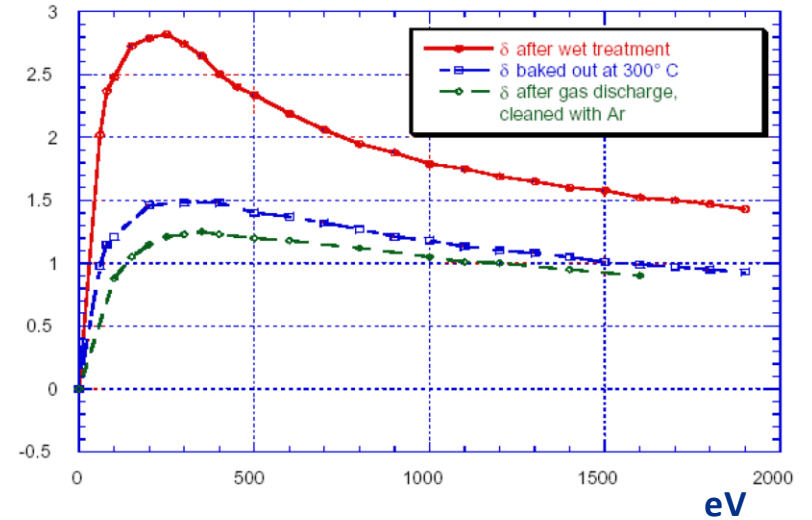


Multipactor discharge with an electric field oscillating between two metal electrodes.



Typical one-point multipactor trajectories for orders 1, 2 and 3.

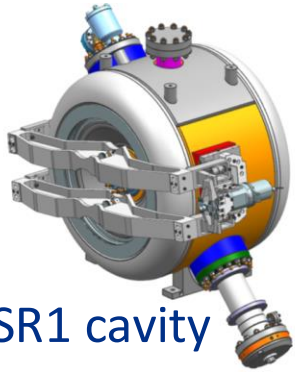
Secondary emission coefficient for Nb



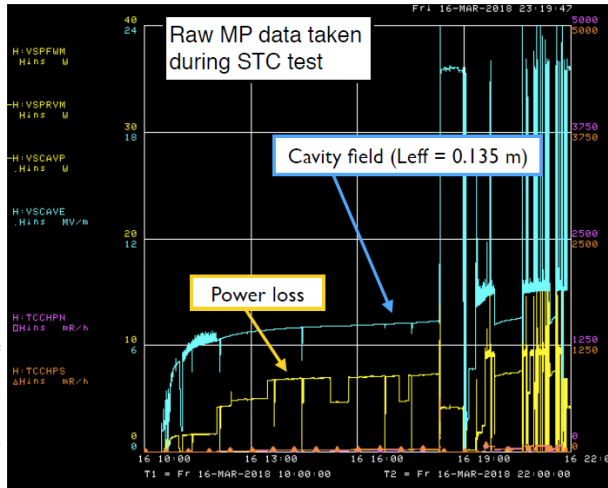
Two point MP in 1.3GHz TESLA cavity. 2D simulations



# Multipacting in SRF cavities



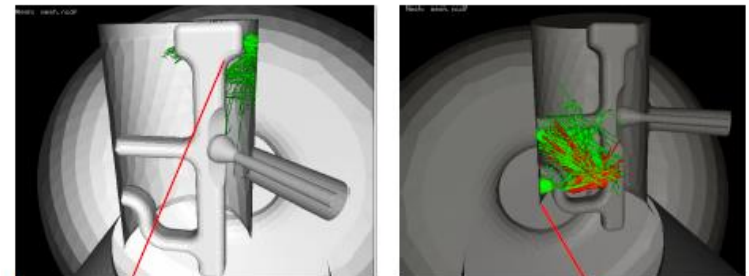
Strong MP in SSR1 at 5, 6.5 and 7 MV/m. 120 C bake for 48 h helps to reduce MP conditioning time



3.9 GHz HOM coupler failure due to overheating caused by MP: redesigned to shift MP barriers above operating gradients



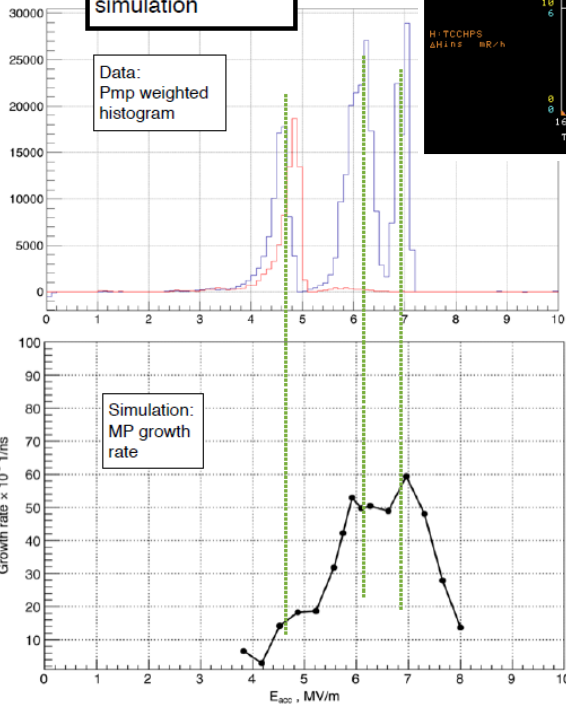
Multipacting in HOM2 at SNS



Comparison to MP simulation

Data: Pmp weighted histogram

Simulation: MP growth rate



- QWR, HWR and SSR are prone to MP, need up to 10 -15 hours to process;
- Elliptical cavities have much better performance.

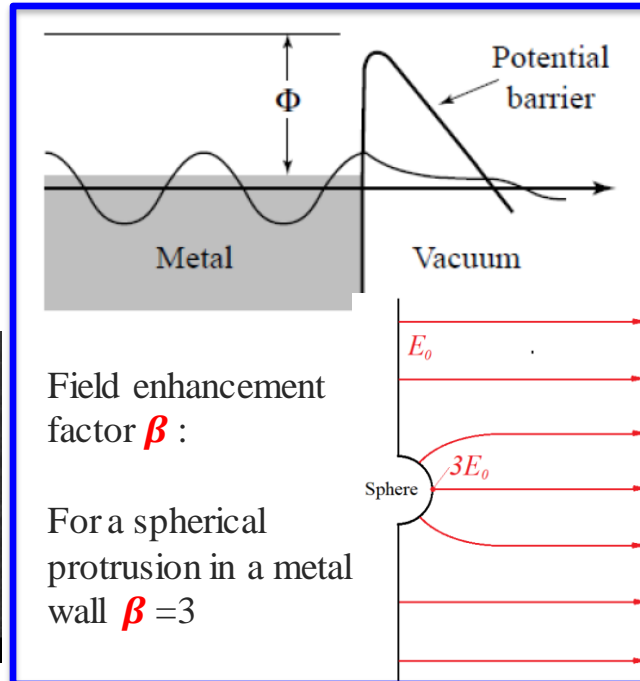
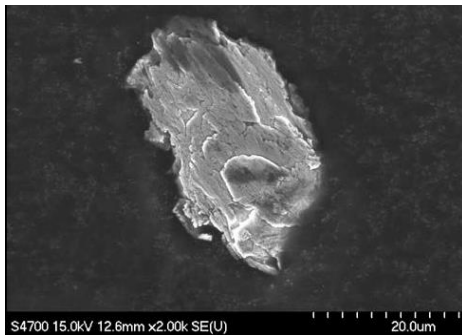
Good agreement between MP conditioning data (Pmp weighted histogram) and MP simulation (growth rate)

# Field emission (FE) and dark currents in SRF cavities

- ❖ FE in SRF cavities is originated from *localized sites* on the inner cavity surface.
- ❖ The predominant source emitters are microscopic particulates adhering to the inner cavity surface, chemical residuals, and geometrical flaws.
  - Field emitters introduced by the necessary chemical surface processing → post chemistry ultrasonic cleaning and high pressure water rising.
  - Field emitters introduced through the cavity opening ports onto the cavity surface, at a time beyond the completion of final cleaning, from external sources → SRF cavities are assembled in large-sized high-quality Class 10 cleanliness clean rooms into cavity strings; critical assembly steps are done with the opening port facing down; cavity strings are evacuated slowly etc.

## ❖ Diagnostics:

- X-ray monitoring/mapping
- Temperature monitoring/mapping
- Electron detecting
- Optical imaging:



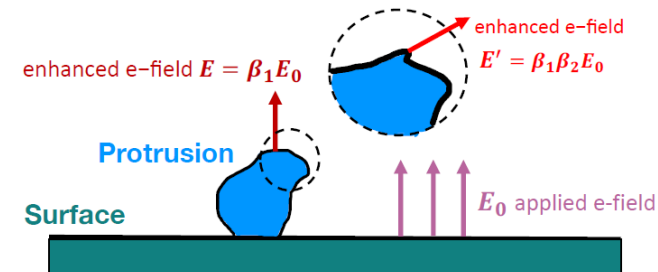
Field enhancement factor  $\beta$  :

For a spherical protrusion in a metal wall  $\beta = 3$

The tunneling current density,  $j(E)$

$$J(E) = k \frac{1.54 \times 10^{-6} (\beta E)^{5/2}}{\Phi} \exp\left(-\frac{6.83 \times 10^9 \Phi^{3/2}}{\beta E}\right)$$

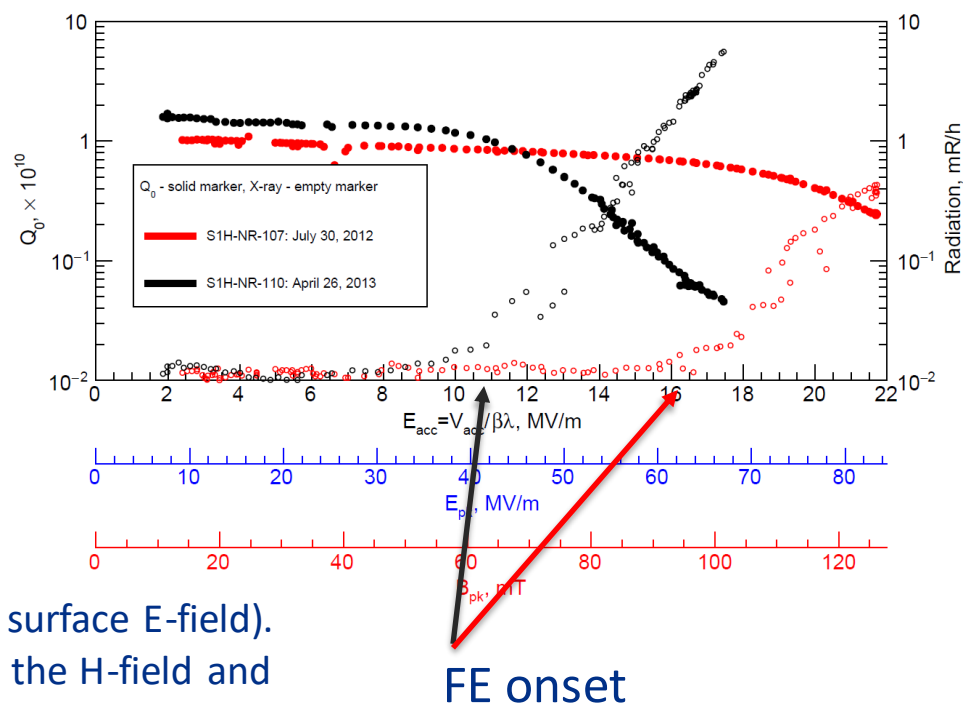
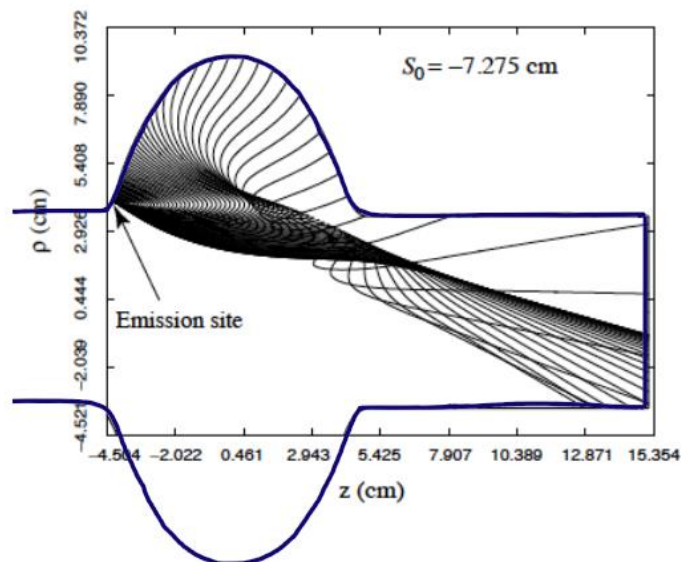
- $j$  – current density in A/m<sup>2</sup>,
- $E$  – surface electric field in MV/m,
- $\Phi$  – work function in eV,
- $\beta$  – field enhancement factor (10-100)
- $k$  – effective emitting surface area.



# Field emission (FE) and dark currents in SRF cavities

## Effect of dark current

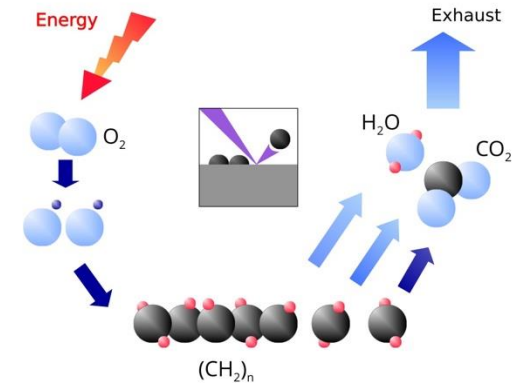
- heat and RF loading of the cavity
- production of avalanches of secondary electrons
- accelerating to hundreds of MeV before being kicked out by down stream quadrupoles
- originating electromagnetic cascade showers in the surrounding materials



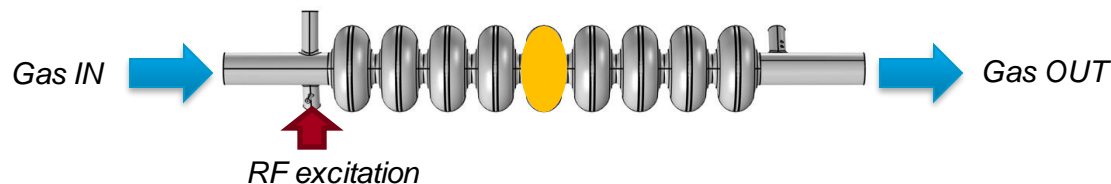
- The emitter is located at the cell entrance (high surface E-field).
- Significant number of FE electrons bend back in the H-field and strike the wall

# In situ field emission mitigation via plasma processing

- While procedures of the cryomodule cavity string assembly are being improved continuously (e.g., R&D on using robotic manipulators), field emission (FE) remains a problem
- Plasma processing was first developed at Oak Ridge National Laboratory
- Gas flow of Ne-O mixture (mostly Ne with a few % of O<sub>2</sub>) at pressure ~ 75-150 mTorr. Argon is used
- Once plasma is ignited, oxygen reacts with hydrocarbons
- Reaction products (mostly CO, CO<sub>2</sub>, H<sub>2</sub>O) are pumped out
- Work function increases, reducing FE
- This method was adapted to LCLS-II and LCLS-II-HE and being investigated for other applications including International Linear Collider
- Recently it was demonstrated that plasma processing helps mitigating multipacting as well



M. Doleans, et al., *Nucl. Instrum. Methods Phys. Res. A* **812**, 50-59 (2016)



P. Berrutti, et al., *J. Appl. Phys.* **126**, 023302 (2019); B. Giaccone et al., *Phys. Rev. Accel. Beams* **24**, 022002 (2021)

# Microphonics and Lorentz Force Detune:

Narrow bandwidth of the cavities caused by low beam loading:

- $Q_{load} = U / (R/Q) / I_{beam}$  - very high for small beam current of few mA,  $Q_{load} \sim 1e7-1e8$ ;
- Cavity bandwidth:  $f / Q_{load} \sim$  tens of Hz.



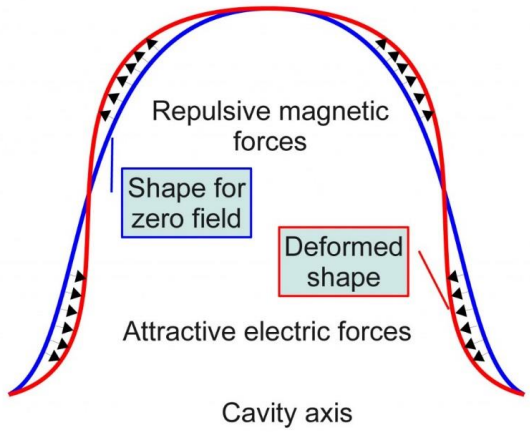
• Pressure variation in the surrounding He bath:

$\Delta f_{He} = df/dP \times \Delta P, \Delta P \sim 0.05-0.1$  mbar at 2 K.  
 $df/dP = 30-130$  Hz/mbar (ILC)

• Internal and external vibration sources (microphonics);

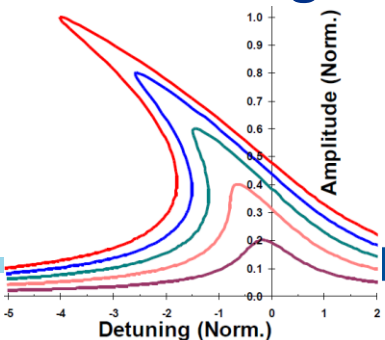
• Radiation pressure from the RF field, Lorentz Force Detuning:

$\Delta f_{LFD} = k_L E^2, k_L$  - Lorentz coefficient,  
 For typical elliptical cavities  $k_L \sim -1$  Hz/(MeV/m)<sup>2</sup>.



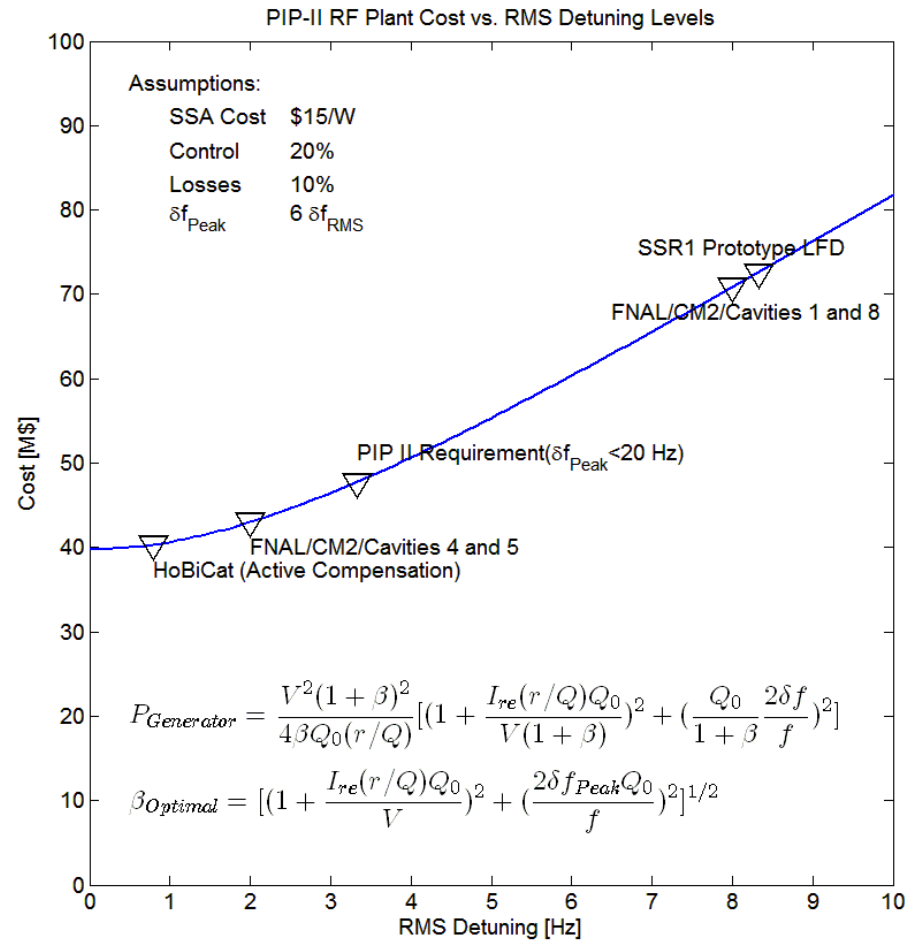
$$P_s = \frac{1}{4} (\mu |\vec{H}|^2 - \epsilon_0 |\vec{E}|^2)$$

$$\Delta f_0 = (f_0)_2 - (f_0)_1 = -K E_{acc}^2$$



# Microphonics:

- Detuned cavities require more RF power to maintain constant gradient
- Providing sufficient reserve increases both the capital cost of the RF plant and the operating cost of the machine
- **PEAK** detuning drives the RF costs
- Beam will be lost if RF reserve is insufficient to overcome PEAK detuning



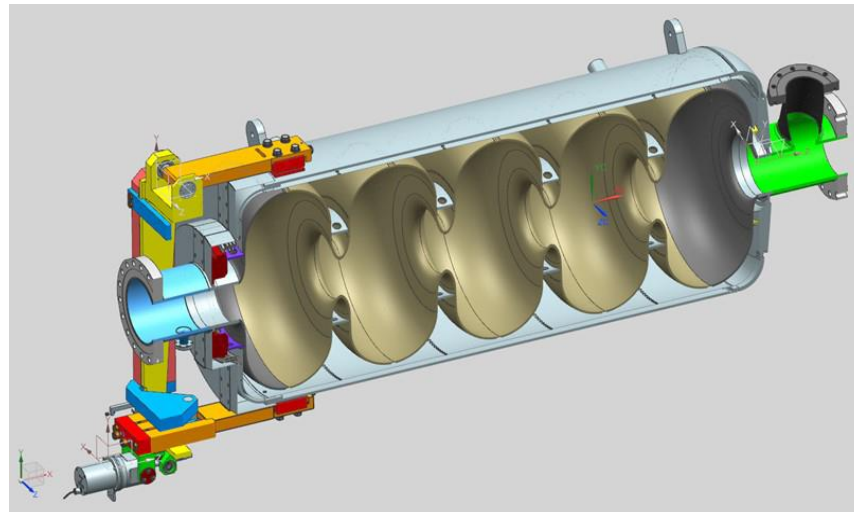


# Microphonics Control Strategies

Microphonics can be mitigated by taking some combination of any or all of the following measures:

- Providing sufficient reserve RF power to compensate for the expected peak detuning levels.
- Improving the regulation of the bath pressure to minimize the magnitude of cyclic variations and transients.
- Reducing the sensitivity of the cavity resonant frequency to variations in the helium bath pressure ( $df/dP$ ).
- Minimizing the acoustic energy transmitted to the cavity by external vibration sources.
- Actively damping cavity vibrations using a fast mechanical or electromagnetic tuner driven by feedback from measurements of the cavity resonant frequency.

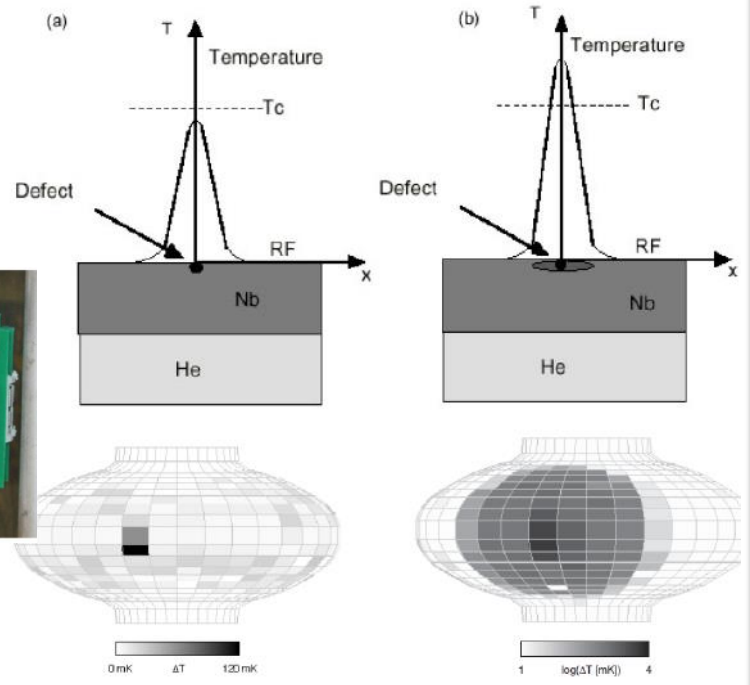
The optimal combination of measures may differ for different cavity types.



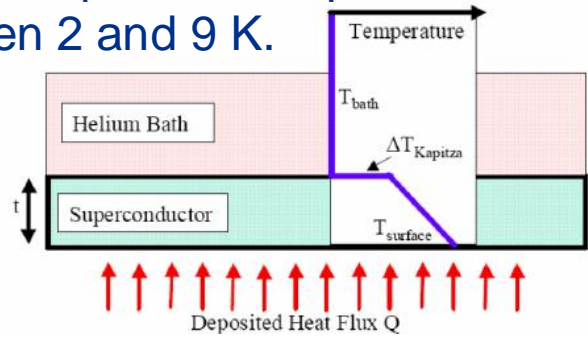
# Thermal breakdown

- If there is a localized heating, the hot area will grow with field. At a certain field there is a thermal runaway and the field collapses (loss of superconductivity or quench).
- Thermal breakdown occurs when the heat generated at the hot spot is larger than that can be evacuated via Nb wall to the helium bath.

Temperature mapping



- Both the thermal conductivity and the surface resistivity of Nb are highly temperature dependent between 2 and 9 K.



$$H_b^2 = \frac{T_0^3}{2 \cdot R_s(T_0) \cdot (\Delta \cdot T_c - T_0)} \cdot \left( \frac{k \cdot h}{k + h \cdot d} \right)$$

$T_0$  - He bath temperature,  
 $T_c$  - critical temperature,  
 $\Delta$  - energy gap,

$h(T_0)$  - Kapitza resistance,  
 $k(T_0)$  - thermal conductivity,

$$R_s(T) = R_0 \cdot \left[ \frac{f(\text{GHz})}{1.3} \right]^2 \cdot \left( \frac{T_c}{T} \right) \cdot e^{-\Delta \cdot \frac{T_c}{T}}$$

$$R_0 = 10^{-5} [\Omega]; \quad \Delta = 1.8; \quad T_c = 9.2^\circ\text{K}$$





# Summary:

- SRF technology allows  $10^6$  less surface losses than RT technology and consequently, much high acceleration gradient at high duty cycle or in CW regime;
- Losses at SRF are determined mainly by BCS resistance (inertia), flux trapping and intrinsic residual resistance;
- The acceleration gradient is limited mainly by thermal breakdown, field emission, etc., but not by breakdown.
- Modern cavity processing techniques (N-doping, etc.) allow very high  $Q_0$ .
- To achieve high  $Q_0$  small residual magnetic field may be required, and therefore, good shielding and degaussing. The cryo-system should allow fast cooling for flux expulsion.
- Resonance discharge (multipacting) may be an issue; cavity processing is required; the cavity shape should be optimized.
- Field emission may limit the gradient; large-scale clean rooms are necessary among other means.